

New Tetraphosphane Ligands $\{(X_2P)_2NC_6H_4N(PX_2)_2\}$ ($X = Cl, F, OMe, OC_6H_4OMe-o$): Synthesis, Derivatization, Group 10 and 11 Metal Complexes and Catalytic Investigations. DFT Calculations on Intermolecular $P \cdots P$ Interactions in Halo-Phosphines

Chelladurai Ganesamoorthy,[†] Maravanji S. Balakrishna,^{*†} Joel T. Mague,[‡] and Heikki M. Tuononen[§]

Phosphorus Laboratory, Department of Chemistry, Indian Institute of Technology Bombay, Mumbai 400 076, India, Department of Chemistry, Tulane University, New Orleans, Louisiana 70118, USA, and Department of Chemistry, P.O. Box 35, FI-40014 University of Jyväskylä, Finland

Received April 23, 2008

The reaction of *p*-phenylenediamine with excess PCl_3 in the presence of pyridine affords $p\text{-C}_6\text{H}_4[\text{N}(\text{PCl}_2)_2]_2$ (**1**) in good yield. Fluorination of **1** with SbF_3 produces $p\text{-C}_6\text{H}_4[\text{N}(\text{PF}_2)_2]_2$ (**2**). The aminotetra(phosphonites) $p\text{-C}_6\text{H}_4[\text{N}\{\text{P}(\text{OC}_6\text{H}_4\text{OMe}-o)_2\}_2]_2$ (**3**) and $p\text{-C}_6\text{H}_4[\text{N}\{\text{P}(\text{OMe})_2\}_2]_2$ (**4**) have been prepared by reacting **1** with appropriate amount of 2-(methoxy)phenol or methanol, respectively, in the presence of triethylamine. The reactions of **3** and **4** with H_2O_2 , elemental sulfur, or selenium afforded the tetrachalcogenides, $p\text{-C}_6\text{H}_4[\text{N}\{\text{P}(\text{O})(\text{OC}_6\text{H}_4\text{OMe}-o)_2\}_2]_2$ (**5**), $p\text{-C}_6\text{H}_4[\text{N}\{\text{P}(\text{S})(\text{OMe})_2\}_2]_2$ (**6**), and $p\text{-C}_6\text{H}_4[\text{N}\{\text{P}(\text{Se})(\text{OMe})_2\}_2]_2$ (**7**) in good yield. Reactions of **3** with $[\text{M}(\text{COD})\text{Cl}_2]$ ($\text{M} = \text{Pd}$ or Pt) ($\text{COD} = \text{cycloocta-1,5-diene}$) resulted in the formation of the chelate complexes, $[\text{M}_2\text{Cl}_4\text{-}p\text{-C}_6\text{H}_4\{\text{N}\{\text{P}(\text{OC}_6\text{H}_4\text{OMe}-o)_2\}_2\}_2]$ (**8**, $\text{M} = \text{Pd}$ and **9**, $\text{M} = \text{Pt}$). The reactions of **3** with 4 equiv of CuX ($X = \text{Br}$ and I) produce the tetranuclear complexes, $[\text{Cu}_4(\mu_2\text{-X})_4(\text{NCCH}_3)_4\text{-}p\text{-C}_6\text{H}_4\{\text{N}\{\text{P}(\text{OC}_6\text{H}_4\text{OMe}-o)_2\}_2\}_2]$ (**10**, $X = \text{Br}$; **11**, $X = \text{I}$). The molecular structures of **1–3**, **6**, **7**, and **9–11** are confirmed by single-crystal X-ray diffraction studies. The weak intermolecular $P \cdots P$ interactions observed in **1** leads to the formation of a 2D sheetlike structure, which is also examined by DFT calculations. The catalytic activity of the $\text{Pd}(\text{II})$ **8** has been investigated in Suzuki–Miyaura cross-coupling reactions.

Introduction

The design and synthesis of polyphosphine ligands has been an active field of research over several years^{1,2} as their metal complexes show structural diversity, high thermal

stability, and unique physical properties.^{3–5} Preorganized ligands of this class may readily form di-, tetra-, and/or polynuclear metal complexes with metals in close proximity

* To whom correspondence should be addressed. E-mail: krishna@chem.iitb.ac.in. Tel.: +91 22 2576 7181. Fax: +91 22 2576 7152/2572 3480.

[†] Indian Institute of Technology Bombay.

[‡] Tulane University.

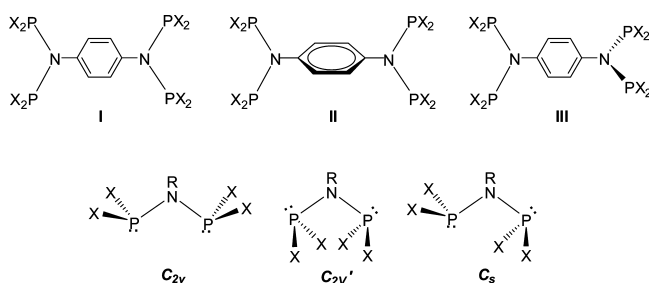
[§] University of Jyväskylä.

- (1) (a) Pei, Y.; Brule, E.; Moberg, C. *Org. Biomol. Chem.* **2006**, *4*, 544–550. (b) Kongprakaiwoot, N.; Luck, R. L.; Urnezus, E. *J. Organomet. Chem.* **2004**, *689*, 3350–3356. (c) Hierso, J.-C.; Fihri, A.; Ivanov, V. V.; Hanquet, B.; Pirio, N.; Donnadiou, B.; Rebiere, B.; Amardeil, R.; Meunier, P. *J. Am. Chem. Soc.* **2004**, *126*, 11077–11087. (d) Hierso, J.-C.; Amardeil, R.; Bentabet, E.; Broussier, R.; Gautheron, B.; Meunier, P.; Kalck, P. *Coord. Chem. Rev.* **2003**, *236*, 143–206. (e) Gaw, K. G.; Smith, M. B.; Steed, J. W. *J. Organomet. Chem.* **2002**, *664*, 294–297. (f) Kuang, S.-M.; Zhang, Z.-Z.; Wang, Q.-G.; Mak, T. C. W. *Inorg. Chem.* **1998**, *37*, 6090–6092.

- (2) (a) Airey, A. L.; Swiegers, G. F.; Willis, A. C.; Wild, S. B. *J. Chem. Soc., Chem. Commun.* **1995**, 695–696. (b) Bianchini, C.; Meli, A.; Peruzzini, M.; Vizza, F.; Zanolini, F. *Coord. Chem. Rev.* **1992**, *120*, 193–208. (c) Cotton, F. A.; Hong, B. *Prog. Inorg. Chem.* **1992**, *40*, 179–289. (d) Caminade, A. M.; Majoral, J. P.; Mathieu, R. *Chem. Rev.* **1991**, *91*, 575–612. (e) Barendt, J. M.; Haltiwanger, R. C.; Squier, C. A.; Norman, A. D. *Inorg. Chem.* **1991**, *30*, 2342–2349. (f) Meek, D. W.; DuBois, D. L.; Tiethof, J. *Adv. Chem. Ser.* **1976**, *150*, 335–357.
- (3) (a) Morisaki, Y.; Ouchi, Y.; Naka, K.; Chujo, Y. *Chem. Asian J.* **2007**, *2*, 1166–1173. (b) Menozzi, E.; Busi, M.; Massera, C.; Ugozzoli, F.; Zuccaccia, D.; Macchioni, A.; Dalcanales, E. *J. Org. Chem.* **2006**, *71*, 2617–2624. (c) Kohl, S. W.; Heinemann, F. W.; Hummert, M.; Bauer, W.; Grohmann, A. *Dalton Trans.* **2006**, 5583–5592. (d) Kohl, S. W.; Heinemann, F. W.; Hummert, M.; Bauer, W.; Grohmann, A. *Chem.–Eur. J.* **2006**, *12*, 4313–4320. (e) Schrauzer, G. N. *Transition Metals in Homogeneous Catalysis*; Marcel Dekker: New York, 1971. (f) Hierso, J.-C.; Beauperin, M.; Meunier, P. *Eur. J. Inorg. Chem.* **2007**, 3767–3780.

to each other, thereby giving rise to strong cooperativity effects in catalytic reactions.⁶ Incorporation of other group 5 and/or group 6 donor atoms into these system results in mixed-multidentate phosphines, which can offer unusual coordination geometry with remarkable chemical behavior at the metal center.⁷ The conformationally rigid polyphosphines of good π -acceptor ligands are potential candidates for designing conducting polymers for effective electronic coupling through ligands.⁸ In addition, their chalcogenide derivatives are more efficient cavitands for the separation of trivalent lanthanides and actinides by solvent-extraction processes compared to the most commonly used dithiophosphinic acids.⁹ However, the methods available for the synthesis of conformationally rigid polyphosphines are mostly multistep and/or low yielding.¹⁰ One of the most commonly known polyphosphines is the tripod ligand $P(CH_2CH_2PR_2)_3$ ($R = Me, Ph$ or cyclohexyl), whose coordination behavior has been extensively studied.^{11,2b} The polyphosphines containing non-carbon spacers are less extensive. The discovery of bis(dihalophosphino)amines, $C1_2P-N(R)-PC1_2$ ($R = alkyl$ or aryl) has resulted in the development of a large number of functionalized bis(phos-

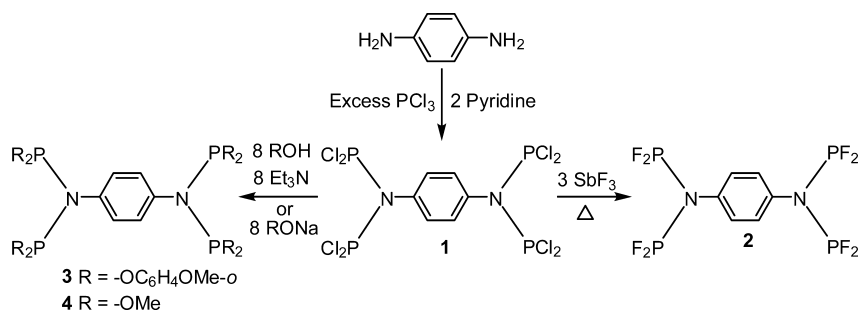
Chart 1



phino)amines of the general formula $R'_2P-N(R)-PR'_2$ ($R' = alkoxide$ or amine).¹² However, the same synthetic methodology is not efficient for the preparation of analogous tetra- and poly(dihalophosphino)amines from aromatic polyamines. The only known tetra(dihalophosphino)amine is $p-C_6H_4[N(PCl_2)_2]_2$ (**1**), which was first synthesized in very low yield (13%) by Haszeldine et al. in 1973, and there is no subsequent follow-up either on its derivatization or its transition-metal chemistry.¹³ Interestingly, the compounds of type **1** can adopt several conformations depending upon the orientation of the P-N-P skeleton with respect to the phenylene ring. Three major idealized possibilities are: (I) both phenylene and P-N-P skeletons can be coplanar, (II) the phenylene ring can be perpendicular to the P-N-P skeleton, and (III) the phenylene and one P-N-P skeleton can be in one plane and orthogonal to the other P-N-P skeleton. Further, the P-N-P moieties in each conformation can adopt C_{2v} , C_{2v}' , and C_s conformations, depending on the mutual orientation of phosphorus lone pairs with respect to the P-substituents as shown in Chart 1,¹⁴ so there is a total of 18 possible conformations.

- (4) (a) Bianchini, C.; Jimenez, M. V.; Meli, A.; Moneti, S.; Vizza, F.; Herrera, V.; Sanchez-Delgado, R. A. *Organometallics* **1995**, *14*, 2342–2352. (b) Bianchini, C.; Meli, A.; Peruzzini, M.; Vizza, F.; Moneti, S.; Herrera, V.; Sanchez-Delgado, R. A. *J. Am. Chem. Soc.* **1994**, *116*, 4370–4381.
- (5) (a) Bruce, D. W. *Adv. Mater.* **1994**, *6*, 699–701. (b) Bruce, D. W.; Holbrey, J. D.; Tajbakhsh, A. R.; Tiddy, G. J. T. *J. Mater. Chem.* **1993**, 905–906.
- (6) (a) Aubry, D. A.; Laneman, S. A.; Fronczek, F. R.; Stanley, G. G. *Inorg. Chem.* **2001**, *40*, 5036–5041. (b) Oro, L. A.; Ciriano, M. A.; Perez-Torrente, J.; Villarroja, B. E. *Coord. Chem. Rev.* **1999**, *193–195*, 941–975. (c) Jiang, H.; Xu, Y.; Liao, S.; Yu, D.; Chen, H.; Li, X. *J. Mol. Catal.* **1999**, *142*, 147–152. (d) Peng, W.-J.; Train, S. G.; Howell, D. K.; Fronczek, F. R.; Stanley, G. G. *Chem. Commun.* **1996**, 2607–2608. (e) Suss-Fink, G. *Angew. Chem., Int. Ed. Engl.* **1994**, *33*, 67–69. (f) Broussard, M. E.; Juma, B.; Train, S. G.; Peng, W.-J.; Laneman, S. A.; Stanley, G. G. *Science* **1993**, *260*, 1784–1788.
- (7) (a) Stossel, P.; Heins, W.; Mayer, H. A.; Fawzi, R.; Steimann, M. *Organometallics* **1996**, *15*, 3393–3403. (b) Uriarte, R.; Mazanec, T. J.; Tau, K. D.; Meek, D. W. *Inorg. Chem.* **1980**, *19*, 79–85.
- (8) (a) Zahavy, E.; Fox, M. A. *Chem.—Eur. J.* **1998**, *4*, 1647–1652. (b) Wang, P.-W.; Fox, M. A. *Inorg. Chem.* **1995**, *34*, 36–41. (c) Wang, P.-W.; Fox, M. A. *Inorg. Chem.* **1994**, *33*, 2938–2945. (d) Wang, P.-W.; Fox, M. A. *Inorg. Chim. Acta* **1994**, *225*, 15–22.
- (9) (a) Boerrigter, H.; Tomasberger, T.; Verboom, W.; Reinhoudt, D. N. *Eur. J. Org. Chem.* **1999**, 665–674. (b) Boerrigter, H.; Verboom, W.; Reinhoudt, D. N. *J. Org. Chem.* **1997**, *62*, 7148–7155. (c) Lobana, T. S. *The Chemistry of Organophosphorus Compounds*; Hartley, F. R., Ed.; Wiley: New York, 1992; Vol. 2, p 1409.
- (10) (a) Gagliardo, M.; Amijs, C. H. M.; Lutz, M.; Spek, A. L.; Havenith, R. W. A.; Hartl, F.; van Klink, G. P. M.; van Koten, G. *Inorg. Chem.* **2007**, *46*, 11133–11144. (b) Yan, Y.; Zhang, X.; Zhang, X. *Adv. Synth. Catal.* **2007**, *349*, 1582–1586. (c) Kondolff, I.; Feuerstein, M.; Doucet, H.; Santelli, M. *Tetrahedron* **2007**, *63*, 9514–9521. (d) Reiter, S. A.; Nogai, S. D.; Schmidbaur, H. Z. *Anorg. Allg. Chem.* **2005**, *631*, 2595–2600. (e) Kim, S.; Kim, J. S.; Kim, S. K.; Suh, I.-H.; Kang, S. O.; Ko, J. *Inorg. Chem.* **2005**, *44*, 1846–1851. (f) Butler, I. R.; Drew, M. G. B.; Caballero, A. G.; Gerner, P.; Greenwell, C. H. *J. Organomet. Chem.* **2003**, *679*, 59–64. (g) Chatterjee, S.; Doyle, R.; Hockless, D. C. R.; Salem, G.; Willis, A. C. *J. Chem. Soc., Dalton Trans.* **2000**, 1829–1830. (h) Steenwinkel, P.; Kolmschot, S.; Gossage, R. A.; Dani, P.; Veldman, N.; Spek, A. L.; van Koten, G. *Eur. J. Inorg. Chem.* **1998**, 477–483. (i) Barney, A. A.; Fanwick, P. E.; Kubiak, C. P. *Organometallics* **1997**, *16*, 1793–1796. (j) Fourmigue, M.; Uzelmeier, C. E.; Boubekour, K.; Bartley, S. L.; Dunbar, K. R. *J. Organomet. Chem.* **1997**, *529*, 343–350. (k) Dieleman, C.; Loeber, C.; Matt, D.; De Cian, A.; Fischer, J. *J. Chem. Soc., Dalton Trans.* **1995**, 3097–3100. (l) Christina, H.; McFarlane, E.; McFarlane, W. *Polyhedron* **1988**, *7*, 1875–1879, and references therein.
- (11) (a) Field, L. D.; Messerle, B. A.; Smernik, R. J.; Hambley, T. W.; Turner, P. *Inorg. Chem.* **1997**, *36*, 2884–2892. (b) Heinekey, D. M.; van Roon, M. *J. Am. Chem. Soc.* **1996**, *118*, 12134–12140. (c) Mayer, H. A.; Kaska, W. C. *Chem. Rev.* **1994**, *94*, 1239–1272. (d) Jia, G.; Drouin, S. D.; Jessop, P. G.; Lough, A. J.; Morris, R. H. *Organometallics* **1993**, *12*, 906–916. (e) Bampos, N.; Field, L. D.; Messerle, B. A.; Smernik, R. J. *Inorg. Chem.* **1993**, *32*, 4084–4088. (f) Bianchini, C. *Pure Appl. Chem.* **1991**, *63*, 829–834. (g) Bampos, N.; Field, L. D. *Inorg. Chem.* **1990**, *29*, 587–588.
- (12) (a) Mandal, S. K.; Venkatakrishnan, T. S.; Sarkar, A.; Krishnamurthy, S. S. *J. Organomet. Chem.* **2006**, *691*, 2969–2977. (b) Veige, A. S.; Gray, T. G.; Nocera, D. G. *Inorg. Chem.* **2005**, *44*, 17–26. (c) Venkatakrishnan, T. S.; Krishnamurthy, S. S.; Nethaji, M. *J. Organomet. Chem.* **2005**, *690*, 4001–4017. (d) Ganesan, M.; Krishnamurthy, S. S.; Nethaji, M. *J. Organomet. Chem.* **2005**, *690*, 1080–1091. (e) Heyduk, A. F.; Nocera, D. G. *J. Am. Chem. Soc.* **2000**, *122*, 9415–9426. (f) Field, J. S.; Haines, R. J.; Stewart, M. W.; Woollam, S. F. *J. Chem. Soc., Dalton Trans.* **1996**, 1031–1037. (g) Edwards, K. J.; Field, J. S.; Haines, R. J.; Homann, B. D.; Stewart, M. W.; Sundermeyer, J.; Woollam, S. F. *J. Chem. Soc., Dalton Trans.* **1996**, 4171–4181. (h) Mague, J. T. *Inorg. Chim. Acta* **1995**, *229*, 17–25. (i) Reddy, V. S.; Katti, K. V.; Barnes, C. L. *Inorg. Chem.* **1995**, *34*, 1273–1277. (j) Balakrishna, M. S.; Reddy, S. V.; Krishnamurthy, S. S.; Nixon, J. F.; St. Laurent, J. C. T. R. B. *Coord. Chem. Rev.* **1994**, *129*, 1–90. (k) King, R. B. *Acc. Chem. Res.* **1980**, *13*, 243–248.
- (13) Davies, A. R.; Dronsfeld, A. T.; Haszeldine, R. N.; Taylor, D. R. *J. Chem. Soc., Perkin Trans. I* **1973**, 379–385.
- (14) (a) Cross, R. J.; Green, T. H.; Keat, R. *J. Chem. Soc., Dalton Trans.* **1976**, 1424–1428. (b) Colquhoun, I. J.; McFarlane, W. *J. Chem. Soc., Dalton Trans.* **1977**, 1674–1679. (c) Keat, R.; Manojlovic-Muir, L.; Muir, K. W.; Rycroft, D. S. *J. Chem. Soc., Dalton Trans.* **1981**, 2192–2198. (d) Prout, T. R.; Imiolczyk, T. W.; Barthelemy, F.; Young, S. M.; Hiltiwanger, R. C.; Norman, A. D. *Inorg. Chem.* **1994**, *33*, 1783–1790. (e) Schmidbaur, H.; Milewski-Mahrla, B.; Muller, G.; Kruger, C. *Organometallics* **1984**, *3*, 38–43. (f) Schmidbaur, H.; Schier, A.; Lauteschlager, S.; Riede, J.; Muller, G. *Organometallics* **1984**, *3*, 1906–1909.

Scheme 1



These conformations can lead to the formation of different types of oligomers and polymers such as linear sheets, twisted chains, or cyclic structures with metals, and the nature of which will depend on the coordination geometry of the transition metals and the possible conformations of the ligand. Further, **1** can also serve as a molecular synthon for producing novel ligands with desired steric and electronic attributes at the phosphorus centers, which may find applications in homogeneous catalysis in addition to interesting coordination chemistry. As a part of our interest in phosphorus-based ligands¹⁵ and their catalytic applications,¹⁶ we describe herein the high-yield synthesis and structural characterization of *p*-C₆H₄[N(PCl₂)₂]₂ (**1**), its reactivity, and group 10 and 11 metal complexes of one of its derivatives *p*-C₆H₄[N{P(OC₆H₄OMe-*o*)₂]₂ (**3**). The utility of the palladium complex [Pd₂Cl₄-*p*-C₆H₄{N{P(OC₆H₄OMe-*o*)₂]₂] (**8**) in Suzuki-Miyaura cross-coupling reactions is also described. Bis-palladium **8** promotes one-pot multiple carbon-carbon coupling reactions very efficiently.

Results and Discussion

Tetraphosphanes. The reaction of *p*-phenylenediamine with phosphorus trichloride in the presence of 2 equiv of pyridine affords the tetraphosphine, *p*-C₆H₄[N(PCl₂)₂]₂ (**1**) in 75% yield. The fluorination of **1** with antimony trifluoride produces the fluoro analogue, *p*-C₆H₄[N(PF₂)₂]₂ (**2**) in 69% yield. **1** and **2** are white crystalline solids, which readily decompose when exposed to air or moisture. **2** is volatile under reduced pressure even at 30 °C. The ³¹P NMR spectrum of **1** consists of a single peak at 153.6 ppm, whereas **2** shows the A portion of an AA'X₂X₂' multiplet centered at 129.7 ppm with ¹J_{PF}, ³J_{PF}, and ²J_{PP} couplings of 1248, 123,

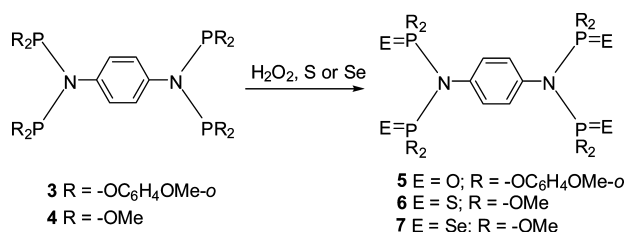
and 392 Hz, respectively.^{14c,17} Tetraphosphine **1** reacts smoothly with the appropriate amount of 2-(methoxy)phenol or methanol in the presence of triethylamine to afford the corresponding tetraphosphonites *p*-C₆H₄[N{P(OC₆H₄OMe-*o*)₂]₂ (**3**) and *p*-C₆H₄[N{P(OMe)₂]₂ (**4**). Treatment of **1** with the sodium salt of 2-(methoxy)phenol in THF also produces **3** in 76% yield as shown in Scheme 1. **3** is an air-stable white crystalline solid, whereas **4** is a white solid with a pungent smell and is moderately stable toward air. The ³¹P NMR spectra of **3** and **4** exhibit single resonances at 132.1 and 134.7 ppm, respectively. The ¹H NMR spectra of the **1–4** show singlets in the range of 7.03–7.79 ppm, corresponding to the protons of the bridging phenylene group. The *o*-methoxy protons in **3** show a singlet at 3.60 ppm, whereas those in **4** resonate as a sharp triplet at 3.51 ppm with a ³J_{PH} coupling of 12.6 Hz. The (EI) mass spectra of **3** and **4** display the molecular ion peaks at *m/z* 1214.47 (*M* + 1) and 477.98 (*M* + 1), respectively. The elemental analyses support the compositions of **1–4** and the structures of **1–3** were confirmed by X-ray structure determination.

Chalcogenide Derivatives. Treatment of **3** with aqueous H₂O₂ (30% w/v) at -78 °C gives the tetra(oxide) derivative, *p*-C₆H₄[N{P(O)(OC₆H₄OMe-*o*)₂]₂ (**5**). A similar oxidation reaction of **3** with S₈ or gray selenium does not proceed even under refluxing conditions in toluene. However, the tetraphosphonite, *p*-C₆H₄[N{P(OMe)₂]₂ (**4**), reacts smoothly with four equivalents of S₈ or gray selenium in toluene under refluxing conditions (32 h) to give the corresponding tetra(sulfide), *p*-C₆H₄[N{P(S)(OMe)₂]₂ (**6**), or tetra(selenide) derivative, *p*-C₆H₄[N{P(Se)(OMe)₂]₂ (**7**). This difference in reactivity may be due to the steric congestion in and the less basic nature of **3** when compared to **4**. However, the reaction of **4** with aqueous H₂O₂ (30% w/v) resulted in the hydrolysis of P-N bonds. The ³¹P NMR spectra of the chalcogenide derivatives **5–7** show singlets at -12.5, 68.8, and 73.4 ppm, respectively. The selenide derivative **7** shows characteristic selenium satellites with a ¹J_{PSe} coupling of 945 Hz. In contrast to **4**, the proton NMR spectra of **6** and **7** show broad doublets for the O-methyl groups at 3.51 and 3.72 ppm with ³J_{PH} couplings of 14.4 and 14.7 Hz, respectively. The (EI) mass spectra of compounds **5–7** display the molecular ion peaks at *m/z* 1278.87 (*M* + 1), 605.15 (*M* + 1), and 794.62 (*M* + 2), respectively, with appropriate isotopic patterns. The structure and com-

- (15) (a) Venkateswaran, R.; Balakrishna, M. S.; Mobin, S. M.; Tuononen, H. M. *Inorg. Chem.* **2007**, *46*, 6535–6541. (b) Ganesamoorthy, C.; Balakrishna, M. S.; Mague, J. T.; Tuononen, H. M. *Inorg. Chem.* **2008**, *47*, 2764–2776. (c) Ganesamoorthy, C.; Mague, J. T.; Balakrishna, M. S. *J. Organomet. Chem.* **2007**, *692*, 3400–3408. (d) Suresh, D.; Balakrishna, M. S.; Mague, J. T. *Tetrahedron Lett.* **2007**, *48*, 2283–2285. (e) Balakrishna, M. S.; Mague, J. T. *Organometallics* **2007**, *26*, 4677–4679. (f) Chandrasekaran, P.; Mague, J. T.; Balakrishna, M. S. *Inorg. Chem.* **2006**, *45*, 5893–5897. (g) Chandrasekaran, P.; Mague, J. T.; Balakrishna, M. S. *Organometallics* **2005**, *24*, 3780–3783.
- (16) (a) Mohanty, S.; Suresh, D.; Balakrishna, M. S.; Mague, J. T. *Tetrahedron* **2008**, *64*, 240–247. (b) Punji, B.; Mague, J. T.; Balakrishna, M. S. *Inorg. Chem.* **2007**, *46*, 11316–11327. (c) Venkateswaran, R.; Mague, J. T.; Balakrishna, M. S. *Inorg. Chem.* **2007**, *46*, 809–817. (d) Venkateswaran, R.; Balakrishna, M. S.; Mobin, S. M. *Eur. J. Inorg. Chem.* **2007**, 1930–1938. (e) Punji, B.; Ganesamoorthy, C.; Balakrishna, M. S. *J. Mol. Catal. A: Chem.* **2006**, *259*, 78–83. (f) Punji, B.; Mague, J. T.; Balakrishna, M. S. *Dalton Trans.* **2006**, 1322–1330.

- (17) (a) King, R. B.; Gimeno, J. *Inorg. Chem.* **1978**, *17*, 2390–2395. (b) Nixon, J. F. *J. Chem. Soc. A* **1969**, 1087–1089.

Scheme 2



positions of compounds **5–7** are consistent with the analytical, ^1H NMR, and mass-spectrometric data. The molecular structures of **6** and **7** were confirmed by single-crystal X-ray structure determinations.

Group 10 and 11 Metal Derivatives. **2–4** are potential tetradentate ligands, and it would be interesting to explore their coordination behavior with various transition-metal salts. The air- and moisture-stable ligand **3** has been used for the preparation of group 10 and 11 metal complexes. The reactions of **3** with 2 equiv of $[\text{M}(\text{COD})\text{Cl}_2]$ ($\text{M} = \text{Pd}$ or Pt) ($\text{COD} = \text{cycloocta-1,5-diene}$) in dichloromethane yielded the chelate complexes, $[\text{M}_2\text{Cl}_4\text{-}p\text{-C}_6\text{H}_4\{\text{N}\{\text{P}(\text{OC}_6\text{H}_4\text{OMe-}o)_2\}_2\}_2]$ (**8**, $\text{M} = \text{Pd}$ and **9**, $\text{M} = \text{Pt}$). The ^{31}P NMR spectra of **8** and **9** consist of single resonances at 64.4 and 35.0 ppm, respectively, which are considerably shielded compared to that of the free ligand. The coordination shifts for **8** and **9** are 67.7 and 97.1 ppm, respectively, and the platinum complex exhibits a large $^1J_{\text{PtP}}$ coupling of 5072 Hz, which is consistent with the proposed cis geometry around the platinum center.¹⁸ The ^1H NMR spectra of **8** and **9** show single resonances around 3.60 ppm corresponding to the *o*-methoxy groups attached to the phenyl rings. Further evidence for the molecular composition of **8** and **9** come from the elemental analyses, ^1H NMR data, and the single-crystal X-ray structure of the platinum derivative **9**. The reactions of **3** with 4 equiv of CuX ($\text{X} = \text{Br}$ and I) in acetonitrile lead to the formation of tetranuclear complexes, $[\text{Cu}_4(\mu_2\text{-X})_4(\text{NCCH}_3)_4\text{-}p\text{-C}_6\text{H}_4\{\text{N}\{\text{P}(\text{OC}_6\text{H}_4\text{OMe-}o)_2\}_2\}_2]$ (**10**, $\text{X} = \text{Br}$; **11**, $\text{X} = \text{I}$) (Scheme 3). **10** and **11** are colorless, air stable, crystalline solids, and moderately soluble in organic solvents. The ^{31}P NMR spectra of **10** and **11** show single resonances at 103.8 and 102.6 ppm, respectively. The ^1H NMR spectra of **10** and **11** show single resonances at 2.07 ppm and 3.56 ppm, respectively, for coordinated CH_3CN and *ortho*-methoxy groups present in the phenyl rings. The analytical data are consistent with the proposed structures and the molecular structures of **10** and **11** are confirmed by the single-crystal X-ray diffraction studies. The ^1H and ^{31}P NMR spectral data for **1–11** are given in Table 1.

The Crystal and Molecular Structures of 1–3, 6, 7, and 9–11. Perspective views of the molecular structures of **1–3**, **6**, **7**, and **9–11** with atom numbering schemes are shown in Figures 1–8, respectively. Crystal data and the details of the structure determinations are given in Table 2, whereas selected bond lengths and bond angles are given in Tables 3–5. The molecular structures of **1–3** consist of

discrete $\text{X}_2\text{P-N(R)-PX}_2$ (**1**, $\text{X} = \text{Cl}$; **2**, $\text{X} = \text{F}$ and **3**, $\text{X} = \text{O}$) skeletons having crystallographically imposed centrosymmetry with the C_{2v} conformation. In **2**, there are two independent half-molecules in the asymmetric unit, which differ only slightly in geometry and conformation. In the $\text{X}_2\text{P-N(R)-PX}_2$ (**1**, $\text{X} = \text{Cl}$; **2**, $\text{X} = \text{F}$ and **3**, $\text{X} = \text{O}$) skeletons, the X atoms are disposed approximately equally above and below the P–N–P plane, whereas there is a distorted-pyramidal geometry about the phosphorus centers and a planar environment around the nitrogen centers with the sum of the angles around nitrogen almost 360° in all cases. The observed P–N bond lengths in **1–3** vary from 1.686(2) to 1.707(2) Å and are comparable with those found in the amino bis(phosphine) derivatives, $^i\text{PrN}(\text{PPh}_2)_2$ (1.710 Å),^{14c} $\text{C}_6\text{H}_5\text{N}\{\text{P}(\text{NHPh})_2\}_2$ (1.690 Å),¹⁹ $\text{CH}_3\text{N}\{\text{P}(\text{NC}_4\text{H}_9)_2\}_2$ (1.685(1)–1.699(1) Å),²⁰ $\text{EtN}\{\text{P}(\text{OC}_6\text{H}_3\text{Pr}_2\text{-}2,6)_2\}_2$ (1.674(5) Å), $\text{EtN}\{\text{P}(\text{OC}_6\text{H}_3\text{Me}_2\text{-}2,6)_2\}_2$ (1.693(2) Å),²¹ $\text{MeN}\{\text{P}(\text{OC}_6\text{H}_3\text{Me}_2\text{-}2,6)_2\}_2$ (1.672(1) Å),²² and shorter than those in $\text{C}_6\text{H}_5\text{-N}(\text{PPh}_2)_2$ (1.732(2) Å), *p*- $\text{CNC}_6\text{H}_4\text{N}(\text{PPh}_2)_2$ (1.723(3)–1.732(3) Å), *m*- $\text{CNC}_6\text{H}_4\text{N}(\text{PPh}_2)_2$ (1.746(2) Å).²³ In **1**, the P–Cl bond distances vary from 2.042(1) to 2.057(1) Å.²⁴ The P–N–P angle ($109.47(6)^\circ$) subtended in **1** is smaller than those of **2** ($115.43(8)^\circ$) and **3** ($115.25(9)^\circ$). In **1–3**, the bridging phenylene rings are almost perpendicular to the plane of the P–N–P skeletons with dihedral angles of $88.58(16)^\circ$ (P2–N–P1 vs C1–C3ⁱ for **1**), $89.73(66)^\circ$ and $87.31(66)^\circ$ (P2–N1–P1 vs C1–C3ⁱ and P3–N2–P4 vs C4–C6ⁱ for **2**) and $78.37(19)^\circ$ (P1–N–P2 vs C29–C31ⁱ for **3**), respectively. In addition, **1** shows all phosphorus atoms to have intermolecular $\text{P}\cdots\text{P}$ contacts of 3.539(1) Å, which are 0.061 Å less than the sum of the van der Waals radii and serve to generate a slightly undulating 2D sheet structure parallel to $\{1,0,0\}$. Although, Lewis acid–base acceptor–donor adducts between simple phosphines are known,²⁵ a search of the current Cambridge Crystallographic Database shows only one example^{25a} of a close (3.372 Å) $\text{P}\cdots\text{P}$ contact in any of the 51 structures containing $\{\text{A-PX}_2\}$ ($\text{A} = \text{N}, \text{C}; \text{X} = \text{halogen}$) moieties. A slightly shorter $\text{P}\cdots\text{P}$ separation is seen in the solid-state structure of $(\text{C}_6\text{F}_5)_2\text{PCH}_2\text{P}(\text{C}_6\text{F}_5)_2$, but here the interactions associate the molecules into discrete pairs.^{25d} It is noteworthy that no discussion is given on the observed interactions, which are of van der Waals in nature, and that only 54 examples of close $\text{P}\cdots\text{P}$ contacts between two tricoordinate phosphorus atoms are found in the current version of the Cambridge Crystallographic Database.

(19) Tarassoli, A.; Haltiwanger, R. C.; Norman, A. D. *Inorg. Chem.* **1982**, *21*, 2684–2690.

(20) Gimbert, Y.; Robert, F.; Durif, A.; Averbuch, M.-T.; Kann, N.; Greene, A. E. *J. Org. Chem.* **1999**, *64*, 3492–3497.

(21) Prabusankar, G.; Palanisami, N.; Murugavel, R.; Butcher, R. J. *Dalton Trans.* **2006**, 2140–2146.

(22) Venkatakrishnan, T. S.; Mandal, S. K.; Kannan, R.; Krishnamurthy, S. S.; Nethaji, M. *J. Organomet. Chem.* **2007**, *692*, 1875–1891.

(23) Fei, Z.; Scopelliti, R.; Dyson, P. J. *Dalton Trans.* **2003**, 2772–2779.

(24) Chen, H. J.; Barendt, J. M.; Haltiwanger, R. C.; Hill, T. G.; Norman, A. D. *Phosphorus Sulfur* **1986**, *26*, 155–162.

(25) (a) Kuhn, N.; Fawzi, R.; Steimann, M.; Wiethoff, J. *Chem. Ber.* **1996**, *129*, 479. (b) Holmes, R. R.; Bertaut, E. F. *J. Am. Chem. Soc.* **1958**, *80*, 2980–2983. (c) Müller, G.; Matheus, H.-J.; Winkler, M. Z. *Naturforsch.* **2001**, *56b*, 1155–1162. (d) Marr, A. C.; Nieuwenhuysen, M.; Pollock, C. L.; Saunders, G. C. *Organometallics* **2007**, *26*, 2659–2671.

(18) Balakrishna, M. S.; Santarsiero, B. D.; Cavell, R. G. *Inorg. Chem.* **1994**, *33*, 3079–3084.

Scheme 3

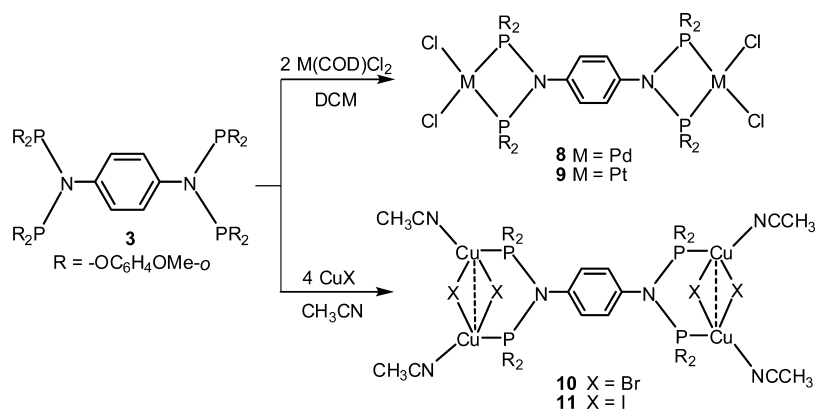


Table 1. NMR Data for 1–11

compounds	$^{31}\text{P}\{^1\text{H}\}$ NMR (in ppm)	^1H NMR (in ppm)		
		CH_3CN	OCH_3	aryl protons
1	153.6 (s)			7.38 (s)
2	129.7 (m) $^1J_{\text{PF}} = 1248$ Hz $^3J_{\text{PF}} = 123$ Hz $^2J_{\text{PP}} = 392$ Hz			7.38 (s)
3	132.1 (s)	3.60 (s)		6.69–7.57 (m)
4	134.7 (s)	3.51 (t) $^3J_{\text{PH}} = 12.6$ Hz		7.03 (s)
5	–12.5 (s)	3.57 (s)		6.70–7.79 (m)
6	68.8 (s)	3.51 (d) $^3J_{\text{PH}} = 14.4$ Hz		7.34 (s)
7	73.4 (s) $^1J_{\text{PSe}} = 945$ Hz	3.72 (d) $^3J_{\text{PH}} = 14.7$ Hz		7.38 (s)
8	64.4 (s)	3.62 (s)		6.78–8.02 (m)
9	35.0 (s) $^1J_{\text{PiP}} = 5072$ Hz	3.60 (s)		6.83–8.03 (m)
10	103.8 (br s)	2.07 (s)	3.57 (s)	6.75–7.66 (m)
11	102.6 (br s)	2.07 (s)	3.55 (s)	6.75–7.74 (m)

In contrast to **1**, no close P...P contacts are observed in its fluoro analogue **2**. Hence, as weak P...P contacts do not appear to be a general feature of the solid-state structures of phosphines bearing electronegative substituents on phosphorus, their occurrence suggests that a fine-tuning of the electronic structure is necessary for this effect to be present. To investigate the phenomenon deeper, theoretical calculations were performed for molecules **1** and **2** as well as for some simplified model systems (below).

The packing of **3** in the solid state is surprisingly efficient, given the bulk of the *o*-methoxyphenoxy substituents and is aided by C–H... π and C–H...O interactions. Thus, H5 is situated 2.92 Å from the center (Cg) of the phenyl ring C15–C20 located at $2 - x, -y, 1 - z$ with a C–H...Cg angle of 144° , whereas H12 is 3.28 Å from Cg of the ring C1–C6 located at $-0.5 + x, y, 1.5 - z$ with a C12–H12...Cg angle of 166° . Additionally, O4 makes an O...H–C hydrogen bond with H28a located at $1.5 - x, 0.5 + y, z$ ($\text{O4}\cdots\text{H28a} = 2.56$ Å; $\text{O4}\cdots\text{H28a}-\text{C28} = 139^\circ$), O5 makes one with H28c located at $0.5 + x, 0.5 - y, 1 - z$ ($\text{O5}\cdots\text{H28c} = 2.72$ Å; $\text{O5}\cdots\text{H28c}-\text{C28} = 155^\circ$) and H21c makes one with O7 located at $0.5 + x, 0.5 - y, 1 - z$ ($\text{O7}\cdots\text{H21c} = 2.50$ Å; $\text{O7}\cdots\text{H21c}-\text{C21} = 162^\circ$).

6 and **7** are isomorphous and virtually isostructural with crystallographically imposed centrosymmetry. As observed

in analogous derivatives, **6** and **7** adopt twisted conformations with the P = E (E = S, Se) vectors, making an angle of $107.6(1)^\circ$ with one another.²⁶ The two independent P = E bonds are virtually same [$1.9191(5)$ Å, $1.9191(6)$ Å for **6** and $2.0720(4)$ Å, $2.0718(4)$ Å for **7**]. The observed P = Se bond distances are longer than those found in compound $\text{PhN}\{\text{P}(\text{Se})(\text{OC}_6\text{H}_4\text{OMe-}o)_2\}_2$ ($2.058(6)$ Å) and is reflected in the relatively low $^1J_{\text{Se-P}}$ coupling of **7**.²⁷ The P–N bond distances vary from $1.677(1)$ to $1.687(1)$ Å in both cases. The P–N–P angles in **6** and **7** are $127.64(8)^\circ$ and $127.00(6)^\circ$,

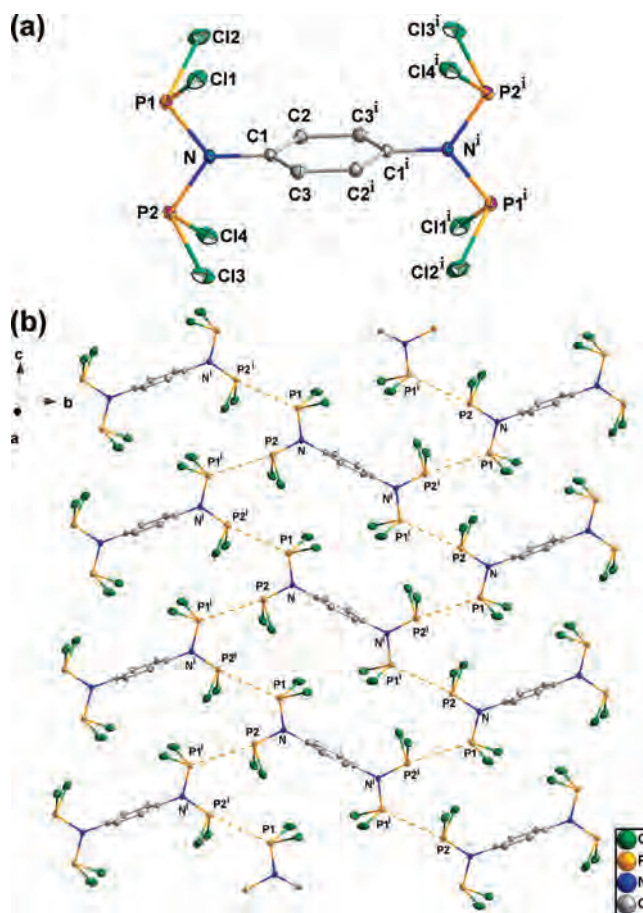


Figure 1. (a) Molecular structure of **1**. All hydrogen atoms have been omitted for clarity. Displacement ellipsoids are drawn at the 50% probability level. Symmetry operation $i = 1 - x, 1 - y, 2 - z$. (b) P...P interaction in **1**. All hydrogen atoms have been omitted for clarity. Displacement ellipsoids are drawn at the 50% probability level.

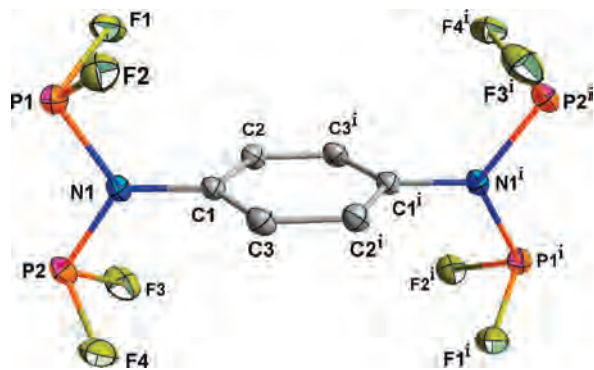


Figure 2. Molecular structure of **2**. All hydrogen atoms have been omitted for clarity. Displacement ellipsoids are drawn at the 50% probability level. Symmetry operation $i = -x, -y, 1 - z$.

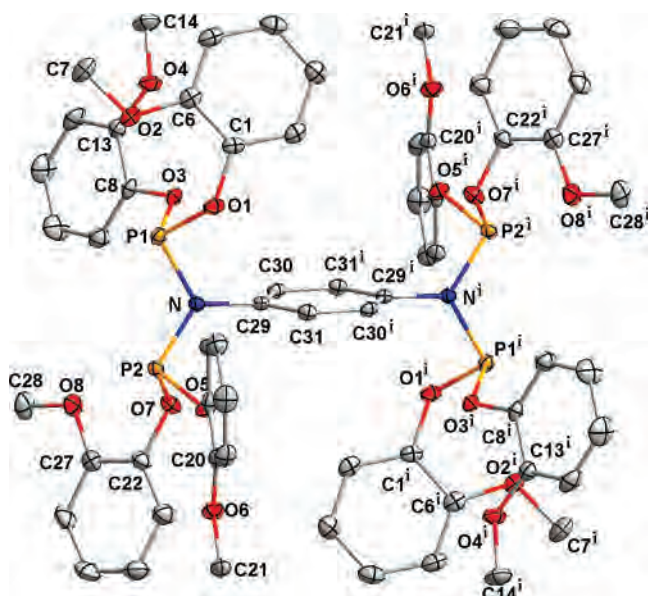


Figure 3. Molecular structure of **3**. All hydrogen atoms have been omitted for clarity. Displacement ellipsoids are drawn at the 50% probability level. Symmetry operation $i = 2 - x, -y, 1 - z$.

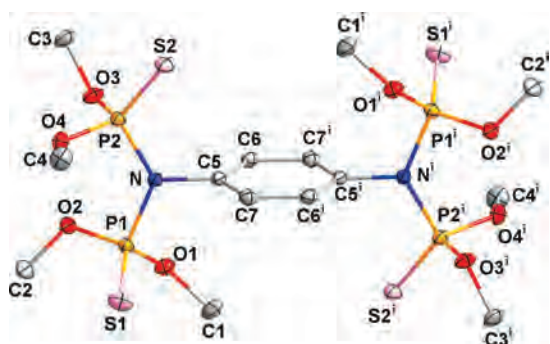


Figure 4. Molecular structure of **6**. All hydrogen atoms have been omitted for clarity. Displacement ellipsoids are drawn at the 50% probability level. Symmetry operation $i = 1/2 - x, 3/2 - y, -z$.

respectively, and are larger than in the free ligands of the type $\text{PhN}\{\text{P}(\text{OR})_2\}$ ($\text{R} = \text{alkyl or aryl groups}$).^{12j} Here again, the bridging phenylene rings are almost perpendicular to the plane of the P-N-P skeletons of **6** and **7** with the dihedral angles of $89.18(14)^\circ$ (P2-N-C5-C6) and $92.16(12)^\circ$ (P2-N-C5-C7), respectively. For both compounds, the molecules pack in sheets parallel to $\{1,0,0\}$ with the sheets assembled through $\text{C-H}\cdots\text{O}$ hydrogen bonding. In **6**, this

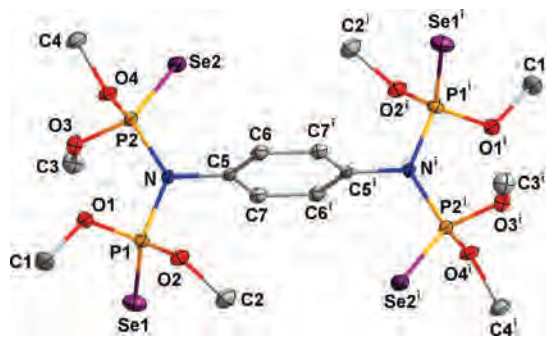


Figure 5. Molecular structure of **7**. All hydrogen atoms have been omitted for clarity. Displacement ellipsoids are drawn at the 50% probability level. Symmetry operation $i = 1/2 - x, 3/2 - y, -z$.

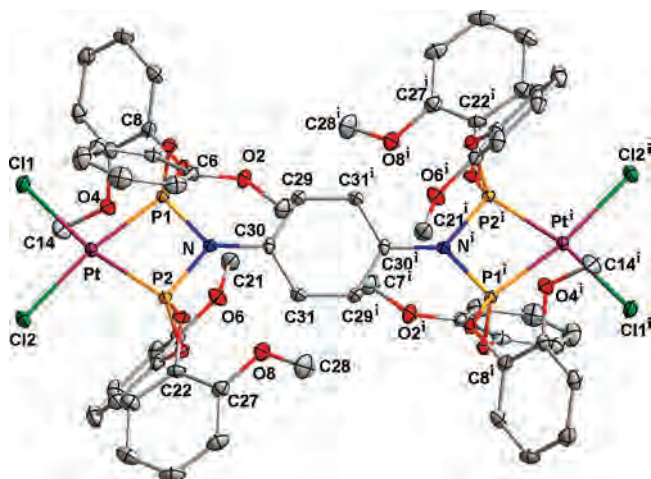


Figure 6. Molecular structure of **9**. All hydrogen atoms and lattice solvents have been omitted for clarity. Displacement ellipsoids are drawn at the 50% probability level. Symmetry operation $i = 1 - x, 2 - y, -z$.

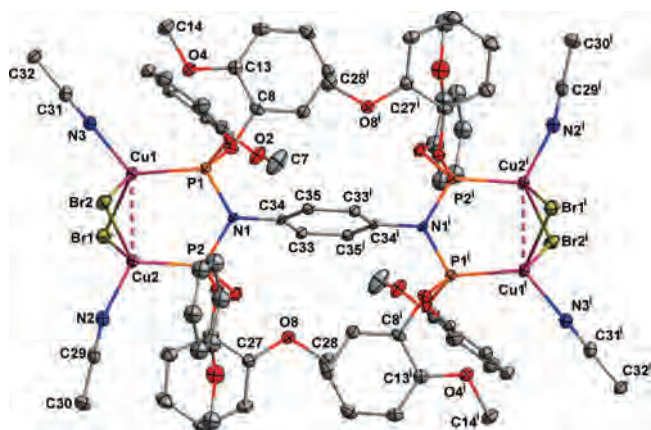


Figure 7. Molecular structure of **10**. All hydrogen atoms and lattice solvents have been omitted for clarity. Displacement ellipsoids are drawn at the 50% probability level. Symmetry operation $i = 1 - x, 1 - y, 2 - z$.

involves $\text{C6-H6}\cdots\text{O4}$ (O4 at $0.5 - x, 0.5 + y, 0.5 - z$; $\text{O4}\cdots\text{H6} = 2.39 \text{ \AA}$; $\text{C6-H6}\cdots\text{O4} = 159^\circ$) and $\text{C4-H4b}\cdots\text{O2}$ (O2 at $0.5 - x, -0.5 + y, 0.5 - z$; $\text{O2}\cdots\text{H4b} = 2.67 \text{ \AA}$; $\text{C4-H4b}\cdots\text{O2} = 156^\circ$), whereas in **7** the interactions are $\text{C6-H6}\cdots\text{O3}$ (O3 at $0.5 - x, -0.5 + y, 0.5 - z$; $\text{O3}\cdots\text{H6} = 2.44 \text{ \AA}$; $\text{C6-H6}\cdots\text{O3} = 160^\circ$) and the weaker, bifurcated hydrogen bond $\text{C3-H3b}\cdots\text{O1, O4}$ (O1 and O4 at $0.5 - x, 0.5 + y, 0.5 - z$); $\text{O1}\cdots\text{H3b} = 2.66 \text{ \AA}$; $\text{O4}\cdots\text{H3b} = 2.64 \text{ \AA}$; $\text{C3-H3b}\cdots\text{O1} = 145^\circ$; $\text{C3-H3b}\cdots\text{O4} = 142^\circ$).

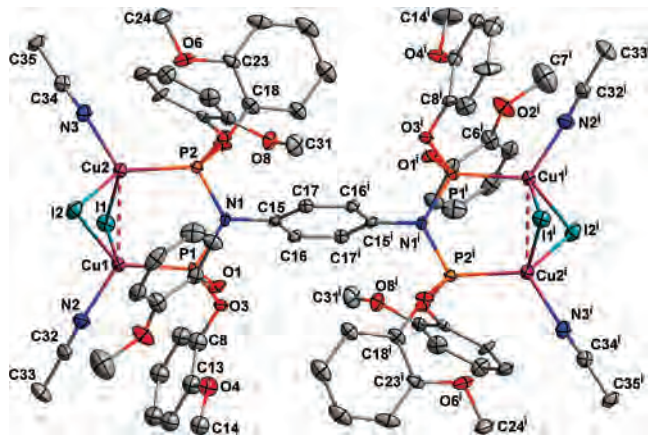


Figure 8. Molecular structure of **11**. All hydrogen atoms and lattice solvent have been omitted for clarity. Displacement ellipsoids are drawn at the 50% probability level. Symmetry operation $i = 2 - x, -y, -z$; $ii = 1 - x, 1 - y, 1 - z$.

The asymmetric unit of **9** contains half a molecule of the metal complex and one molecule of chloroform. The platinum adopts an approximate square-planar geometry, with the corners occupied by two chlorines and two phosphorus atoms of tetraphosphazane **3**. In the molecular structure of **9**, the two independent P–N [P1–N = 1.684(2) Å and P2–N = 1.686(2) Å] and P–Pt [P1–Pt = 2.177(1) Å and P2–Pt = 2.179(1) Å] distances are virtually the same, whereas the P–N–P angle shrinks from 115.25(9) to 97.46(9)° due to the formation of a strained four-membered chelate ring. The P1–Pt–P2, Cl1–Pt–Cl2, Cl1–Pt–P1, and Cl2–Pt–P2 bond angles are 71.12(2)°, 90.92(2)°, 97.75(2)°, and 100.22(2)°, respectively, which show the distortion in the square-planar geometry. In contrast to the molecular structures of **1–3**, **6**, and **7**, the bridging phenylene ring is almost parallel to the plane produced by P1–N–P2 skeleton with the dihedral angle of 0.7(3)° (P2–N–C30–C21). Molecules of **9** appear to be associated via C–H...O hydrogen bonding involving one phenoxy group on each side of the ligand viz. C24–H24...O1 and C25–H25...O2 (O1 and O2 at $1 + x, y, z$; H24...O1 = 2.70 Å; C24–H24...O1 = 176°; H25...O2 = 2.71 Å; C25–H25...O2 = 130°).

The molecular structures of **10** and **11** consist of discrete Cu_2X_2 core (**10**, X = Br and **11**, X = I) having crystallographically imposed centrosymmetry. In **11**, there are two independent half-molecules in the asymmetric unit, which differ only slightly in geometry and conformation with both the molecules has been held together by weak C–H...I and C–H...C interactions. All of the copper(I) centers are tetrahedrally coordinated to a phosphorus atom, two bridging halides, and a solvent molecule. As observed in complexes $\text{Cu}_2(\mu_2\text{-I})_2(\text{NCCH}_3)_2\{\mu\text{-PhN}(\text{P}(\text{OC}_6\text{H}_4\text{OME-}o)_2)_2\}$ and $\text{Cu}_2(\mu_2\text{-D})_2(\text{C}_5\text{H}_5\text{N})_2\{\mu\text{-PhN}(\text{P}(\text{OC}_6\text{H}_4\text{OME-}o)_2)_2\}$,²⁸ the Cu_2X_2 core adopts a butterfly shape with the halide atoms at the wingtips. The four Cu–X bond lengths differ significantly from one

- (26) Hitchcock, P. B.; Nixon, J. F.; Silaghi-Dumitrescu, I.; Haiduc, I. *Inorg. Chim. Acta* **1985**, *96*, 77–80.
 (27) Balakrishna, M. S.; George, P. P.; Mague, J. T. *J. Organomet. Chem.* **2004**, *689*, 3388–3394.
 (28) Ganesamoorthy, C.; Balakrishna, M. S.; George, P. P.; Mague, J. T. *Inorg. Chem.* **2007**, *46*, 848–858.

Table 2. Crystallographic Information for **1–3**, **6**, **7**, and **9–11**

	1	2	3	6	7	9	10	11
empirical formula	$\text{C}_6\text{H}_4\text{Cl}_2\text{N}_2\text{O}_6\text{P}_4$	$\text{C}_6\text{H}_4\text{F}_8\text{N}_2\text{P}_4$	$\text{C}_6\text{H}_6\text{N}_2\text{O}_{16}\text{P}_4$	$\text{C}_{14}\text{H}_{28}\text{N}_2\text{O}_8\text{P}_4\text{S}_4$	$\text{C}_{14}\text{H}_{28}\text{N}_2\text{O}_8\text{P}_4\text{Se}_4$	$\text{C}_{64}\text{H}_{62}\text{Cl}_{10}\text{N}_2\text{O}_{16}\text{P}_4\text{Pt}_2$	$\text{C}_{74}\text{H}_{78}\text{Br}_4\text{Cu}_4\text{N}_8\text{O}_{16}\text{P}_4$	$\text{C}_{74}\text{H}_{78}\text{Cu}_4\text{I}_4\text{N}_8\text{O}_{16}\text{P}_4$
fw	511.59	379.99	1213.00	604.54	792.10	1983.70	2033.12	2221.13
cryst syst	monoclinic	triclinic	orthorhombic	monoclinic	monoclinic	monoclinic	triclinic	triclinic
space group	$P2_1/c$ (no. 14)	$P\bar{1}$ (no. 2)	$Pbca$ (no. 61)	$C2/c$ (no. 15)	$C2/c$ (no. 15)	$P2_1/n$ (no. 14)	$P\bar{1}$ (no. 2)	$P\bar{1}$ (no. 2)
a , Å	6.3127(5)	7.7034(6)	15.611(2)	17.167(1)	17.386(2)	10.589(1)	9.8172(6)	10.120(1)
b , Å	20.286(2)	8.8807(7)	17.516(2)	10.542(1)	10.552(1)	18.440(1)	13.6523(8)	13.781(1)
c , Å	7.603(1)	9.9791(8)	21.384(2)	14.584(1)	14.822(2)	19.093(1)	16.417(1)	31.671(3)
α , deg	90	84.503(1)	90	90	90	90	107.528(1)	98.402(1)
β , deg	113.502(1)	88.234(1)	90	93.930(1)	93.753(2)	98.047(1)	98.468(1)	92.990(1)
γ , deg	90	88.808(1)	90	90	90	90	97.337(1)	98.442(1)
V , Å ³	892.93(13)	679.11(9)	5847.3(11)	2633.3(3)	2713.4(5)	3691.7(4)	2040.5(2)	4310.0(7)
Z	2	2	4	4	4	2	2	2
ρ_{calc} , g cm ⁻³	1.903	1.858	1.378	1.525	1.939	1.785	1.655	1.712
μ (Mo K α), mm ⁻¹	1.607	0.637	0.202	0.645	5.684	4.299	3.133	2.546
$F(000)$	500	372	2536	1256	1544	1948	1022	2188
T (K)	100	100	100	100	100	100	100	200
2θ range, deg	3.1–28.3	2.3–28.2	2.0–27.1	2.3–28.3	2.3–28.3	2.1–28.3	2.3–28.3	1.3–25.0
total no. reflns	15 494	11 932	91 509	22 671	40 527	64 668	36 417	31 953
no. of indep reflns	2220	3309	6471	3266	6839	9168	10 031	14 276
GOF (F^2)	[$R_{\text{int}} = 0.022$]	[$R_{\text{int}} = 0.024$]	[$R_{\text{int}} = 0.073$]	[$R_{\text{int}} = 0.031$]	[$R_{\text{int}} = 0.054$]	[$R_{\text{int}} = 0.034$]	[$R_{\text{int}} = 0.038$]	[$R_{\text{int}} = 0.045$]
R_{int}^a	1.091	1.13	1.09	1.06	0.92	1.06	1.04	1.15
wR_{int}^b	0.0213	0.0263	0.0484	0.0297	0.0385	0.0197	0.0339	0.0501
wR_2^b	0.0518	0.0750	0.1118	0.0779	0.0947	0.0474	0.0841	0.1179
$a^c R = \sum F_o - F_c / \sum F_o $								
$b^c R_w = \{[\sum w(F_o - F_c)^2] / \sum w(F_o)^2\}^{1/2}$								

Table 3. Selected Bond Distances and Bond Angles for **1–3**

1				2				3			
bond distances (angstroms)		bond angles (degrees)		bond distances (angstroms)		bond angles (degrees)		bond distances (angstroms)		bond angles (degrees)	
C11–P1	2.0457(5)	C11–P1–C12	98.51(2)	F1–P1	1.582(1)	F1–P1–F2	94.43(6)	P1–N	1.707(2)	P1–N–P2	115.25(9)
C12–P1	2.0421(5)	C13–P2–C14	98.28(2)	F2–P1	1.586(1)	F3–P2–F4	94.52(7)	P2–N	1.694(2)	O1–P1–N	94.59(7)
C13–P2	2.0574(5)	P1–N–P2	109.47(6)	F3–P2	1.575(1)	P1–N–P2	115.43(8)	P1–O1	1.639(1)	O3–P1–N	101.91(7)
C14–P2	2.0547(5)	C11–P1–N	101.53(4)	F4–P2	1.584(1)	F1–P1–N1	99.62(6)	P1–O3	1.642(1)	O5–P2–N	101.83(7)
P1–N	1.704(1)	C12–P1–N	102.31(4)	P1–N1	1.689(1)	F2–P1–N1	98.90(6)	P2–O5	1.648(1)	O7–P2–N	97.02(7)
P2–N	1.703(1)	C13–P2–N	101.69(4)	P2–N1	1.686(2)	F3–P2–N1	99.39(7)	P2–O7	1.636(1)	O1–P1–O3	95.43(7)
N–C1	1.445(2)	C14–P2–N	101.73(4)	N–C1	1.453(2)	F4–P2–N1	99.88(7)	N–C29	1.445(2)	O5–P2–O7	95.04(7)
P2⋯P1 _{i(inter)}	3.539(1)	P1–N–C1	124.69(9)			P1–N1–C1	121.3(1)			P1–N–C29	120.51(1)
P2⋯P1 _{i(intra)}	7.620	P2–N–C1	125.82(9)			P2–N1–C1	123.3(1)			P2–N–C29	124.05(1)
P1⋯P2	2.781										

Table 4. Selected Bond Distances and Bond Angles for **6, 7, and 9**

6				7				9			
bond distances (angstroms)		bond angles (degrees)		bond distances (angstroms)		bond angles (degrees)		bond distances (angstroms)		bond angles (degrees)	
P1–N	1.684(1)	P1–N–P2	127.64(8)	Se1–P1	2.072(1)	P1–N–P2	127.00(6)	P1–N	1.684(2)	P1–N–P2	97.46(9)
P2–N	1.677(1)	S1–P1–O1	114.32(4)	Se2–P2	2.072(1)	Se1–P1–O1	117.40(4)	P2–N	1.686(2)	C11–Pt–Cl2	90.92(2)
S1–P1	1.919(1)	S1–P1–O2	117.60(5)	P1–N	1.687(1)	Se1–P1–O2	114.50(4)	Pt–P1	2.177(1)	C11–Pt–P1	97.75(2)
S2–P2	1.919(1)	S2–P2–O3	116.67(5)	P2–N	1.680(1)	Se2–P2–O3	116.02(3)	Pt–P2	2.179(1)	Cl2–Pt–P2	100.22(2)
P1–O1	1.579(1)	S2–P2–O4	115.94(4)	P1–O1	1.566(1)	Se2–P2–O4	116.43(4)	Pt–Cl1	2.340(1)	C11–Pt–P2	168.87(2)
P1–O2	1.568(1)	O1–P1–O2	102.34(6)	P1–O2	1.581(1)	O1–P1–O2	102.44(5)	Pt–Cl2	2.354(1)	Cl2–Pt–P1	171.31(2)
P2–O3	1.576(1)	O3–P2–O4	101.39(6)	P2–O3	1.574(1)	O3–P2–O4	101.49(4)	P1–O1	1.596(2)	P1–Pt–P2	71.12(2)
P2–O4	1.577(1)	S1–P1–N	116.05(5)	P2–O4	1.572(1)	Se1–P1–N	115.94(4)	P1–O3	1.579(2)	O1–P1–O3	100.30(8)
N–C5	1.454(2)	S2–P2–N	113.55(5)	N–C5	1.454(2)	Se2–P2–N	113.95(4)	P2–O5	1.582(2)	O5–P2–O7	101.13(8)
		P1–N–C5	113.99(9)			P1–N–C5	114.19(8)	P2–O7	1.580(2)	Pt–P1–O1	119.35(6)
		P2–N–C5	118.20(9)			P2–N–C5	118.66(8)	N–C30	1.435(3)	Pt–P1–O3	124.90(6)
										Pt–P2–O5	122.35(6)
										Pt–P2–O7	122.79(6)

Table 5. Selected Bond Distances and Bond Angles for **10 and 11**

10				11			
bond distances (angstroms)		bond angles (degrees)		bond distances (angstroms)		bond angles (degrees)	
P1–N1	1.694(13)	P1–N1–P2	119.6(7)	P1–N1	1.709(8)	P1–N1–P2	119.0(4)
P2–N1	1.687(13)	N1–P1–Cu1	114.8(5)	P2–N1	1.709(8)	N1–P1–Cu1	116.5(3)
P1–O1	1.626(12)	N1–P2–Cu2	118.6(5)	P1–O1	1.626(7)	N1–P2–Cu2	116.0(3)
P1–O3	1.623(11)	P1–Cu1–Br1	112.60(14)	P1–O3	1.610(7)	P1–Cu1–I1	105.25(7)
P2–O5	1.627(11)	P1–Cu1–Br2	110.15(13)	P2–O5	1.614(7)	P1–Cu1–I2	115.80(8)
P2–O7	1.624(12)	P2–Cu2–Br1	96.97(13)	P2–O7	1.635(7)	P2–Cu2–I1	104.27(8)
P1–Cu1	2.191(4)	P2–Cu2–Br2	121.43(14)	P1–Cu1	2.194(3)	P2–Cu2–I2	116.42(8)
P2–Cu2	2.179(4)	P1–Cu1–N3	124.5(4)	P2–Cu2	2.215(3)	P1–Cu1–N2	120.4(3)
Cu1–Br1	2.525(3)	P2–Cu2–N2	116.2(4)	Cu1–I1	2.788(2)	P2–Cu2–N3	119.7(3)
Cu1–Br2	2.554(3)	Cu1–Br1–Cu2	64.93(7)	Cu1–I2	2.629(2)	Cu1–I1–Cu2	59.07(4)
Cu2–Br1	2.582(3)	Cu1–Br2–Cu2	66.63(8)	Cu2–I1	2.688(2)	Cu1–I2–Cu2	61.17(4)
Cu2–Br2	2.435(3)	Br1–Cu1–Br2	100.08(9)	Cu2–I2	2.678(2)	I1–Cu1–I2	106.08(5)
Cu1–N3	1.995(14)	Br1–Cu2–Br2	101.74(9)	Cu1–N2	1.980(10)	I1–Cu2–I2	107.59(5)
Cu2–N2	1.991(14)			Cu2–N3	2.016(10)		

another but can be seen (Table 5) to fall roughly into a longer pair and a shorter pair with each copper atom forming a long and a short Cu–X bond. The distance between the two copper centers in **10** and **11** are 2.742 Å and 2.700 Å (2.730 Å for another half of molecule in the asymmetric unit of **11**), respectively, which indicate the presence of ligand supported Cu⋯Cu interactions.²⁸ In the molecular structures of **10** and **11**, the two independent Cu–P distances differ only slightly (Cu1–P1 = 2.191(4) Å and Cu2–P2 = 2.179(4) Å for **10** and Cu1–P1 = 2.194(3) Å and Cu2–P2 = 2.215(3) Å for **11**), whereas the X–Cu–X angles (Br1–Cu1–Br2 = 100.08(9)° and Br1–Cu2–Br2 = 101.74(9)° for **10**; I1–Cu1–I2 = 106.08(5)° and I1–Cu2–I2 = 107.59(5)° for **11**) show the distortion in the tetrahedral environment around copper atoms. The angles about the

halide atoms (Cu1–Br1–Cu2 = 64.93(7)° and Cu1–Br2–Cu2 = 66.63(8)° for **10**; Cu1–I1–Cu2 = 59.07(4)° and Cu1–I2–Cu2 = 61.17(4)° for **11**) are considerably smaller. The torsion angles observed between bridging phenylene ring with P–N–P plane are 80.0(17)° (P1–N–P2 vs C34–C35) for **10** and 77.4(10)° (P1–N–P2 vs C15–C16) for **11**.

DFT Calculations on P⋯P Interactions in **1** and **2**

DFT calculations were first performed for dimers of **1** and **2** at the PBE1PBE/TZVP level of theory. The geometries were fully optimized within C_{2h} symmetry, and the resulting metrical parameters are in excellent agreement with their experimental counterparts. Selected average bond lengths and bond angles are **1**: $r(\text{P–Cl}) = 2.081$ Å, $r(\text{P–N}) = 1.726$ Å, $r(\text{N–C}) = 1.429$ Å, $\angle\text{PNP} = 109.6^\circ$, **2**: $r(\text{P–F}) = 1.612$ Å, $r(\text{P–N}) = 1.714$ Å, $r(\text{N–C}) = 1.436$ Å, $\angle\text{PNP} = 115.0^\circ$.

The calculated intermolecular P...P contact is 3.591 Å and 3.774 Å in **1** and **2**, respectively. The calculated interaction energy (including counterpoise correction) is only -2 kJ mol^{-1} for **1** and virtually nonexistent for **2**.

Taking into account the known difficulties of the standard density functionals in modeling weak interactions and van der Waals forces in particular,²⁹ the geometries and energies obtained for **1** and **2** should be compared with data from calculations employing correlated wave function methods such as Möller–Plesset perturbation theory (MP) or coupled cluster (CC). Unfortunately the systems under study are somewhat large to be treated at either above levels of theory, which makes accurate calculations time-consuming. Hence, we carried out MP2 calculations only for model systems for which we used the weakly bonded PX_3 dimers ($\text{X} = \text{F}, \text{Cl}$) in C_{2h} symmetry. The smaller size of the molecules facilitates the usage of considerably larger basis sets, which in turn helps to remove computational errors arising from basis set incompleteness (basis set superposition error, BSSE). Because MP2 is more prone to BSSE than DFT, counterpoise correction was applied throughout the MP2 geometry optimizations. For comparison purposes, the model systems were also calculated with DFT using the PBE1PBE functional in combination with the aug-cc-pVTZ basis sets.

At the MP2/aug-cc-pVTZ level of theory, the predicted P...P distance for $\text{Cl}_3\text{P}\cdots\text{PCl}_3$ is 3.266 Å, that is, 0.334 Å shorter than the sum of van der Waals radii. In contrast, the C_{2h} symmetric structure for the fluoro derivative has a considerably longer P...P separation of 3.887 Å, which indicates the absence of any bonding interaction. Concomitantly, the calculated MP2 interaction energies (with counterpoise correction) are -15 kJ mol^{-1} and -1 kJ mol^{-1} for $\text{Cl}_3\text{P}\cdots\text{PCl}_3$ and $\text{F}_3\text{P}\cdots\text{PF}_3$, respectively. DFT calculations for the model systems yielded intermolecular P...P contacts of 3.580 and 3.736 Å and interaction energies of -2 and -1 kJ mol^{-1} for the chloro and fluoro derivatives, respectively. This data is in excellent agreement with the values obtained for systems **1** and **2** (above). Interestingly, the C_{2h} symmetric structure of $\text{F}_3\text{P}\cdots\text{PF}_3$ is not a minimum on the potential energy hypersurface but a first-order transition state. Subsequent optimization following the transition state vector gives a true minimum (all frequencies real) which is C_2 symmetric and has an even longer P...P separation of 3.801 Å. An analogous C_2 symmetric structure with a P...P distance of 3.888 Å could also be located using the MP2/aug-cc-pVTZ Hamiltonian. However, the energy of the C_2 conformer is on par with the C_{2h} structure at both DFT and MP2 levels of theory. Hence, we conclude that the two monomers in the van der Waals dimer $\text{F}_3\text{P}\cdots\text{PF}_3$ are practically noninteracting.

Taken as a whole, the computational results not only confirm the presence of weak van der Waals interactions between two N-PX_2 moieties but also demonstrate that the interaction strength is dependent on the identity of the atoms attached to the nuclei. The interactions are practically absent in fluoro **2**, whereas their presence in the analogous chloro

derivative **1** suffices to create an ordered supramolecular assembly of molecules in the crystal lattice. The calculated DFT and MP2 results represent upper and lower limits for the interaction energy, respectively. Thus, the binding energy in $\text{Cl}_3\text{P}\cdots\text{PCl}_3$ is approximated to be around $5-10 \text{ kJ mol}^{-1}$. We note that analogous short (less than sum of van der Waals radii) contacts between tricoordinate group 15 atoms have been observed previously for example in Cp^*AsI_2 ³⁰ and in the 2:1 complex between SbCl_3 and 1,3,5-triacetylbenzene.³¹ In addition, spectroscopic studies of liquid and solid PBr_3 have indicated the formation of ethane-like dimers $\text{Br}_3\text{P}=\text{PBr}_3$ on transition to crystalline state.³² Hence, a more exhaustive study of the nature of bonding interactions in $\text{X}_3\text{E}\cdots\text{EX}_3$ systems ($\text{E} = \text{pnictogen}, \text{X} = \text{halogen}$) using highly accurate wave functions seems warranted.³³ A full report on the conducted computational investigations will be given in due course.³⁴

Suzuki–Miyaura cross-coupling reactions. The palladium-catalyzed Suzuki–Miyaura cross-coupling reaction is one of the efficient methods for forming symmetric and nonsymmetric biaryl compounds in organic synthesis.³⁵ Pd(II) **8** effectively catalyzes the Suzuki–Miyaura cross-coupling reactions of a variety of aryl halides with phenylboronic acid to afford the desired biaryls in remarkably high yields (Table 6). These reactions were studied systematically to find the optimal conditions to afford biaryls in good yield. It is important to achieve good yields using minimum amounts of catalyst, therefore we examined the effect of catalyst loading on the coupling between 4-bromobenzonitrile and phenylboronic acid. Complete conversion of the starting materials into biphenyl-4-carbonitrile was achieved with 0.5 mol% of catalyst in 1 h or 0.2 mol% in 4 h, therefore a concentration of 0.2 mol% was selected as the optimal concentration for catalytic loading. The Suzuki–Miyaura cross-coupling reaction is strongly influenced by the solvent and base. Whereas the reactions proceed with various bases (K_3PO_4 , KF, Et_3N , etc.) or solvents (THF, DCM, toluene), the best results were obtained with either potassium carbonate or cesium carbonate as the base and methanol as the solvent. Therefore, the catalytic reactions have been carried out in methanol (5 mL) with potassium carbonate as a base. For

(29) See, for example: Koch, W.; Holthausen, M. C. *A Chemist's Guide to Density Functional Theory*; VCH: Weinheim, 2001.

(30) Avtomonov, E. V.; Megges, K.; Wocadlo, S.; Lorberth, J. *J. Organomet. Chem.* **1996**, *524*, 253–261.

(31) Baker, W. A.; Williams, D. E. *Acta Crystallogr., Sect. B.* **1978**, *34*, 3739–3741.

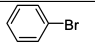
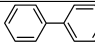
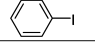
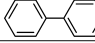
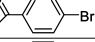
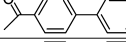
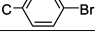
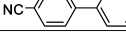
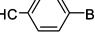
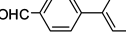
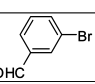
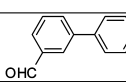

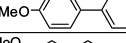
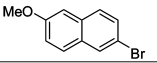
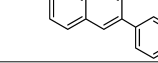
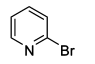
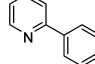
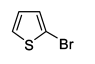
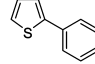
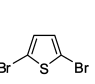
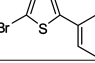
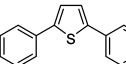
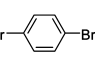
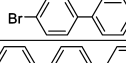
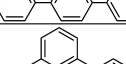
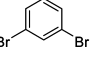

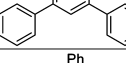
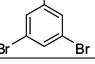
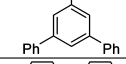
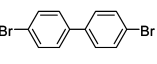
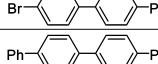
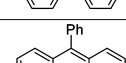
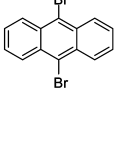
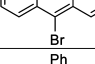
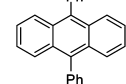
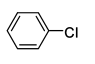
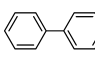
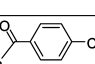
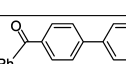
(32) Kozulin, A. T.; Gogolev, A. V.; Karmanov, V. I.; Murstovkin, V. A. *USSR. Opt. Spektrosk.* **1973**, *34*, 1218.

(33) We are aware of only three theoretical publications discussing weak P...P interactions in phosphine dimers (a) Del Bene, J. E.; Frisch, M. J.; Pople, J. A. *J. Phys. Chem.* **1985**, *89*, 3669–3674. (b) Altmann, J. A.; Govender, M. G.; Ford, T. A. *Mol. Phys.* **2005**, *103*, 949–961. (c) Wang, W.; Zheng, W.; Pu, X.; Wong, N.-B.; Tian, A. *J. Mol. Struct.* **2003**, *625*, 25–30.

(34) Tuononen, H. M.; Balakrishna, M. S., manuscript in preparation.

(35) (a) Miyaura, N.; Suzuki, A. *Chem. Rev.* **1995**, *95*, 2457–2483. (b) Chemler, S. R.; Trauner, D.; Danishefsky, S. J. *Angew. Chem., Int. Ed.* **2001**, *40*, 4544–4568. (c) Hassan, J.; Sevignon, M.; Gozzi, C.; Schulz, E.; Lemaire, M. *Chem. Rev.* **2002**, *102*, 1359–1469. (d) Kotha, S.; Lahiri, K.; Kashinath, D. *Tetrahedron* **2002**, *58*, 9633–9695. (e) Littke, A. F.; Fu, G. C. *Angew. Chem., Int. Ed.* **2002**, *41*, 4176–4211. (f) Zapf, A.; Beller, M. *Chem. Commun.* **2005**, 431–440. (g) Phan, N. T. S.; Sluys, M. V. D.; Jones, C. W. *Adv. Synth. Catal.* **2006**, *348*, 609–679. (h) Weng, Z.; Teo, S.; Hor, T. S. A. *Acc. Chem. Res.* **2007**, *40*, 676–684.

Table 6. Suzuki–Miyaura Cross-Coupling Reactions of Aryl Halides with Phenylboronic Acid Catalyzed by [Pd₂Cl₄-p-C₆H₄{N{P(OC₆H₄OMe-o)₂}₂}₂] (**8**)^{a,b,c}

Entry	Aryl Halide	Product	Condition ^a	Conv. [%] ^b	TON ^c
1			0.2 mol%. R.T., 1 h	97	485
2			0.2 mol%. R.T., 2 h	96	480
3			0.2 mol%. R.T., 1/2 h	96	480
4			0.2 mol%. R.T., 4 h	99	495
5			0.2 mol%. R.T., 1 h	85	425
			0.1 mol%. Reflux, 1 h	100	1000
6			0.2 mol%. R.T., 1 h	86	430
7			0.2 mol%. R.T., 12 h	100	500
8			0.2 mol%. R.T., 4 h	90	450
9			0.5 mol%. R.T., 4 h	41	82
10			0.2 mol%. R.T., 24 h	80	400
11			0.2 mol%. R.T., 48 h	15	210
				27	
12			0.2 mol%. R.T., 2 h	2	500
				98	
13			0.2 mol%. R.T., 4 h	2	500
				98	
14			0.2 mol%. R.T., 24 h	100	500
15			0.2 mol%. R.T., 1 h	17	385
				60	
16			0.2 mol%. R.T., 24 h	0.2	476
				95	
17			0.2 mol%. R.T., 12 h	5	25
			1 mol%. Reflux, 10 h	100	100
18			1 mol%. Reflux, 10 h	70	70

^a Aryl halide (0.5 mmol), phenylboronic acid (0.75, 1.25, and 1.75 mmol for mono-, di- and tribromo derivatives, respectively), K₂CO₃ (1 mmol), MeOH (5 mL). ^b Conversion to a coupled product determined by GC, based on aryl halides; average of two runs. ^c Defined as mol product per mol of catalyst.

example, bromo- or iodobenzene and phenylboronic acid in the presence of K₂CO₃ shows 97% conversion in methanol

at room temperature with 0.2 mol% of catalyst within 1–2 h (Table 6, entries 1 and 2). **8** proved to be an active catalyst for both the easy-to-couple substrate 4-bromoacetophenone and the more challenging, electronically deactivated substrate 4-bromoanisole. Higher conversion rates were realized when activated aryl bromides were used as substrates (Table 6, entries 3 and 4). Even though good conversions were observed with deactivated and sterically bulky aryl bromides (Table 6, entries 7 and 8) low catalytic conversions were observed with heterocyclic bromides (Table 6, entries 9–11). In addition, the cross-coupling reactions of a number of di- and tribromobenzenes with phenylboronic acid were examined. As shown in Table 6, the dibromobenzenes including those with sterically bulky aryl bromides gave high di/monosubstituted product ratios (entries 12–16). Coupling reactions performed with 1,3- and 1,4-dibromobenzene yielded 98% of disubstituted terphenyls and 2% of monosubstituted bromobiphenyls after 2–4 h with the complete consumption of the dibromobenzenes. A gradual increase in the yield of terphenyl was observed with time, and a maximum of 99.6% conversion into 1,1':3',1''-terphenyl was achieved after 12 h (Table 6, entry 13). In the case of coupling reactions with 4,4'-dibromobiphenyl and 9,10-dibromoanthracene, 60:17 and 95:0.2 ratios of di/monosubstituted derivatives were obtained with in a period of 24 h with a small amount of unreacted starting materials. The rate of conversion of 9,10-dibromoanthracene is faster than 4,4'-dibromobiphenyl, and no improvement in the conversions have been observed in both the cases after attaining a particular period of time. Also, because of the solubility problem the reactions were carried out in toluene (Table 6, entries 15 and 16).

The catalytic activity of **8** toward aryl chlorides was also examined and found to be relatively unreactive toward the less expensive aryl chlorides at room temperature with low catalyst loading. For example, the coupling reaction of chlorobenzene with phenylboronic acid afforded only 5% of the conversion product with 0.2 mol% of catalyst at room temperature. However, complete conversion of chlorobenzene into biphenyl was observed at reflux temperature with 1 mol% catalyst loading (Table 6, entry 17). In the case of activated and deactivated aryl chlorides, the catalytic system becomes inactive over time (30–35% conversion) and the deposition of palladium particles is seen.

Poisoning experiments were carried out with metallic mercury to test for the presence of a palladium colloid.³⁶ When a drop of Hg(0) was added to the coupling reaction of 4-bromoacetophenone with phenylboronic acid at the start, the catalytic activity was not suppressed. This shows the homogeneous nature of the catalyst because heterogeneous catalysts would form an amalgam, thereby poisoning it.

Conclusion

The aminotetra(phosphines) **1–4** have been prepared in moderate to good yield from *p*-phenylenediamine. **1** can

(36) (a) Widegren, J. A.; Bennett, M. A.; Finke, R. G. *J. Am. Chem. Soc.* **2003**, *125*, 10301–10310. (b) Widegren, J. A.; Finke, R. G. *J. Mol. Catal. A: Chem.* **2003**, *198*, 317–341.

serve as a molecular synthon for producing large number of tetra- and multidentate phosphines with different steric and electronic properties based on the choice of nucleophiles. The chloro derivative **1** shows intermolecular P...P interactions whose strength is estimated to be around -5 to -10 kJ mol^{-1} using computational methods. In agreement with the calculated data, similar interactions are virtually absent in the fluoro derivative **2**. Hence, the results of this study indicate that when using appropriate substituents, P...P interactions – in spite of their weakness – can be utilized for example in building supramolecular assemblies or in crystal engineering. The oxidation behavior of **3** and **4** toward chalcogens differ due to the difference in steric and Lewis basic nature of the phosphorus centers. The group 10 and 11 metal complexes are moderately stable toward air and moisture. Pd(II) **8** is an efficient catalyst for the coupling of several activated and deactivated aryl bromides and chlorides with phenylboronic acid and also for the one-pot multiple carbon–carbon couplings at room temperature. The tetra-phosphanes can show up to 18 conformational isomers. It would be interesting to analyze the relative stabilities of these conformers and to explore their potential ability to form complexes with various transition-metal derivatives. Further organometallic chemistry and catalytic reactions with this system is under active investigation in our laboratory.

Experimental Section

General Procedures. All manipulations were performed under rigorously anaerobic conditions using Schlenk techniques. All the solvents were purified by conventional procedures and distilled prior to use.³⁷ The compounds $[\text{M}(\text{COD})\text{Cl}_2]$ ($\text{M} = \text{Pd}$ and Pt)^{38a} and CuBr ^{38b} were prepared according to the published procedures. Pyrazine, phenylboronic acid, 2-bromo-6-methoxynaphthalene, 9,10-dibromoanthracene, 1,3-dibromobenzene, 1,4-dibromobenzene, 4,4'-dibromobiphenyl, 1,3,5-tribromobenzene, and 2,5-dibromothiophene were purchased from Aldrich chemicals and used as such. Other chemicals were obtained from commercial sources and purified prior to use.

Instrumentation. The ^1H and $^{31}\text{P}\{^1\text{H}\}$ NMR (δ in ppm) spectra were recorded using a Varian VXR 300 or VXR 400 spectrometer operating at the appropriate frequencies using TMS and 85% H_3PO_4 as internal and external references, respectively. The microanalyses were performed using a Carlo Erba Model 1112 elemental analyzer. Electro-spray ionization (EI) mass spectrometry experiments were carried out using Waters Q-ToF micro-YA-105. GC analyses were performed on a PerkinElmer Clarus 500 GC fitted with packed column. The melting points were observed in capillary tubes and are uncorrected.

Synthesis of $p\text{-C}_6\text{H}_4[\text{N}(\text{PCl}_2)_2]_2$ (1**).** Pyridine (5.85 g, 0.074 mol) was added dropwise to a mixture of p -phenylenediamine (4.0 g, 0.037 mol) and PCl_3 (75 mL) at -78 °C with constant stirring. The resultant suspension was slowly warmed to room temperature,

refluxed for 2 days, and filtered through a frit. The insoluble residue was extracted with hot PCl_3 (2×15 mL). The combined extracts were concentrated to half and kept at -30 °C for 1 day to give analytically pure product of **1** as white crystals. Yield: 75% (14.2 g). Mp: 118–120 °C (dec). Anal. Calcd for $\text{C}_6\text{H}_4\text{Cl}_8\text{N}_2\text{P}_4$: C, 14.08; H, 0.79; N, 5.48. Found: C, 14.14; H, 0.77; N, 5.44%. ^1H NMR (300 MHz, CDCl_3): δ 7.38 (s, *Ph*, 4H). $^{31}\text{P}\{^1\text{H}\}$ NMR (121 MHz, CDCl_3): δ 153.6 (s).

Synthesis of $p\text{-C}_6\text{H}_4[\text{N}(\text{PF}_2)_2]_2$ (2**).** A mixture of **1** (1.288 g, 2.517 mmol) and SbF_3 (1.350 g, 7.551 mmol) was heated to reflux in toluene (30 mL) for 24 h. It was then cooled to room temperature, filtered, and the solvent was removed under reduced pressure to give a sticky residue. The residue was extracted with CH_2Cl_2 (3×7 mL) and the combined extracts were concentrated to 5 mL. The solution was layered with 1 mL of *n*-hexane and stored at -30 °C for 2 days to afford **2** as a white crystalline material. The crystals suitable for X-ray diffraction analysis were grown by subliming a small quantity of **2** in a thin capillary tube at 50–52 °C under reduced pressure (0.05 mmHg). Yield: 69% (0.660 g). Anal. Calcd for $\text{C}_6\text{H}_4\text{F}_8\text{N}_2\text{P}_4$: C, 18.96; H, 1.06; N, 7.37. Found: C, 19.01; H, 1.14; N, 7.42%. ^1H NMR (400 MHz, CDCl_3): δ 7.38 (s, *Ph*, 4H). $^{31}\text{P}\{^1\text{H}\}$ NMR (162 MHz, CDCl_3): δ 129.7 (m, $^1J_{\text{PF}} = 1248$ Hz, $^3J_{\text{PF}} = 123$ Hz and $^2J_{\text{PP}} = 392$ Hz).

Synthesis of $p\text{-C}_6\text{H}_4[\text{N}\{\text{P}(\text{OC}_6\text{H}_4\text{OMe-}o)_2\}]_2$ (3**).** Method 1: A mixture of *o*-methoxyphenol (6.92 g, 6.2 mL, 0.056 mol) and Et_3N (5.64 g, 7.8 mL, 0.056 mol) in 20 mL of toluene was added dropwise over 15 min to a well-stirred toluene solution (100 mL) of **1** (3.58 g, 0.007 mol) at 0 °C. The reaction mixture was stirred for 12 h at room temperature and refluxed for 4 h. The hot solution was filtered through a heated frit and then stored at room temperature for a day to afford **3** as white crystals. Additional product could be separated from the amine hydrochloride by washing the filter cake successively with water, methanol, and diethylether (10 mL each). Yield: 84% (7.13 g).

Method 2: Freshly distilled *o*-methoxyphenol (7.06 g, 6.3 mL, 0.057 mol) and sodium (1.31 g, 0.057 mol) were taken in 50 mL of THF in a two-necked flask topped with a reflux condenser and a dropping funnel. The reaction mixture was refluxed for 6 h and then allowed to cool to room temperature. A solution of **1** (3.64 g, 0.007 mol) in THF (60 mL) was transferred to the dropping funnel through a cannula and was added dropwise to the reaction mixture at 0 °C. The reaction mixture was further stirred for 12 h at room temperature and then filtered through a frit. The filtrate was concentrated to 30 mL under reduced pressure and stored at -30 °C to afford analytically pure product of **3** as a white crystalline material. Yield: 76% (6.55 g). Mp: 128–130 °C. Anal. Calcd for $\text{C}_{62}\text{H}_{60}\text{N}_2\text{O}_{16}\text{P}_4$: C, 61.39; H, 4.98; N, 2.31. Found: C, 61.31; H, 4.99; N, 2.30%. ^1H NMR (400 MHz, CDCl_3): δ 7.57–6.69 (m, *Ph*, 36H), 3.60 (s, *OCH}_3*, 24H). $^{31}\text{P}\{^1\text{H}\}$ NMR (162 MHz, CDCl_3): δ 132.1 (s). MS (EI): 1214.47 ($m/z + 1$).

Synthesis of $p\text{-C}_6\text{H}_4[\text{N}\{\text{P}(\text{OMe})_2\}]_2$ (4**).** A mixture of methanol (1.01 g, 1.3 mL, 0.031 mol) and Et_3N (3.17 g, 4.4 mL, 0.031 mol) in 20 mL of toluene was added dropwise over 15 min to a well-stirred toluene solution (40 mL) of **1** (1.95 g, 3.82 mmol) at 0 °C. The reaction mixture was stirred for 24 h at room temperature. The amine hydrochloride was removed by filtration through a frit and the filtrate was concentrated to 10 mL under reduced pressure and stored at -30 °C to afford **4** as a white crystalline material. Yield: 52% (0.946 g). Mp: 96–98 °C. Anal. Calcd for $\text{C}_{14}\text{H}_{28}\text{N}_2\text{O}_8\text{P}_4$: C, 35.30; H, 5.92; N, 5.88. Found: C, 35.31; H, 5.99; N, 5.80%. ^1H NMR (400 MHz, CDCl_3): δ 7.03 (s, *Ph*, 4H), 3.51 (t, *OCH}_3*, $^3J_{\text{PH}} = 12.6$ Hz, 24H). $^{31}\text{P}\{^1\text{H}\}$ NMR (162 MHz, CDCl_3): δ 134.7 (s). MS (EI): 477.98 ($m/z + 1$).

(37) Armarego, W. L. F.; Perrin, D. D. *Purification of Laboratory Chemicals*, 4th ed.; Butterworth-Heinemann: Linacre House, Jordan Hill, Oxford, U.K., 1996.

(38) (a) Drew, D.; Doyle, J. R. *Inorg. Synth.* **1990**, 28, 346. (b) Furniss, B. S.; Hannaford, A. J.; Smith, P. W. G.; Tatchell, A. R. *Vogel's Textbook of Practical Organic Chemistry*, 5th ed.; ELBS: England 1989; pp 428–429.

(39) (a) *SMART, version 5.625*; Bruker-AXS: Madison, WI, 2000. (b) *APEX2, Version 2.1–4*; Bruker-AXS: Madison, WI, 2007.

Synthesis of p -C₆H₄[N{P(O)(OC₆H₄OMe-*o*)₂]₂]₂ (5**).** A 30% aqueous solution of H₂O₂ (0.022 g, 0.07 mL, 0.654 mmol) in THF (7 mL) was added dropwise to a well-stirred THF solution (10 mL) of **3** (0.189 g, 0.156 mmol) at -78 °C. The reaction mixture was slowly warmed to room temperature and stirred for 5 h. The solvent was removed under reduced pressure to give a sticky residue. The residue was dissolved in 5 mL of CH₂Cl₂, layered with 1 mL of *n*-hexane and kept at -30 °C to afford **5** as an analytically pure brown crystalline product. Yield: 70% (0.139 g). Mp: 194–196 °C. Anal. Calcd for C₆₂H₆₀N₂O₂₀P₄: C, 58.31; H, 4.74; N, 2.19. Found: C, 58.25; H, 4.79; N, 2.20%. ¹H NMR (400 MHz, CDCl₃): δ 7.79–6.70 (m, *Ph*, 36H), 3.57 (s, *OCH*₃, 24H). ³¹P{¹H} NMR (162 MHz, CDCl₃): δ -12.5 (s). MS (EI): 1278.87 (*m/z* + 1).

Synthesis of p -C₆H₄[N{P(S)(OMe)₂]₂]₂ (6**).** A mixture of **4** (0.105 g, 0.222 mmol) and elemental sulfur (0.030 g, 0.930 mmol) in 15 mL of toluene was refluxed for 30 h. The solution was cooled to room temperature and filtered to remove unreacted sulfur. The solvent was removed under reduced pressure to give a white residue. The residue was dissolved in 4 mL of CH₂Cl₂, layered with 1 mL of *n*-hexane and stored at -30 °C for 2 days to afford analytically pure white crystals of **6**. Yield: 77% (0.103 g). Mp: 164–166 °C. Anal. Calcd for C₁₄H₂₈N₂O₈P₄S₄: C, 27.81; H, 4.67; N, 4.63; S, 21.22. Found: C, 27.75; H, 4.63; N, 4.58; S, 21.20%. ¹H NMR (400 MHz, CDCl₃): δ 7.34 (s, *Ph*, 4H), 3.51 (d, *OCH*₃, ³J_{PH} = 14.4 Hz, 24H). ³¹P{¹H} NMR (162 MHz, CDCl₃): δ 68.8 (s). MS (EI): 605.15 (*m/z* + 1).

Synthesis of p -C₆H₄[N{P(Se)(OMe)₂]₂]₂ (7**).** This was synthesized by a procedure similar to that of **6** using **4** (0.106 g, 0.224 mmol) and elemental selenium (0.074 g, 0.941 mmol). Yield: 82% (0.146 g). Mp: 168–170 °C. Anal. Calcd for C₁₄H₂₈N₂O₈P₄Se₄: C, 21.23; H, 3.56; N, 3.54. Found: C, 21.20; H, 3.47; N, 3.60%. ¹H NMR (300 MHz, CDCl₃): δ 7.38 (s, *Ph*, 4H), 3.72 (d, *OCH*₃, ³J_{PH} = 14.7 Hz, 24H). ³¹P{¹H} NMR (121 MHz, CDCl₃): δ 73.4 (s, ¹J_{PSe} = 945 Hz). MS (EI): 794.62 (*m/z* + 2).

Synthesis of [Pd₂Cl₄- p -C₆H₄[N{P(OC₆H₄OMe-*o*)₂]₂]₂ (8**).** A solution of [Pd(COD)Cl₂] (0.040 g, 0.139 mmol) in 10 mL of CH₂Cl₂ was added dropwise to a solution of **3** (0.084 g, 0.069 mmol) also in CH₂Cl₂ (7 mL). The reaction mixture was allowed to stir at room temperature for 5 h to give clear-yellow solution. The solution was concentrated to 5 mL, saturated with 3 mL of *n*-hexane, and stored at -30 °C for 1 day to give an analytically pure yellow crystalline product **8**. Yield: 70% (0.076 g). Mp: 186–188 °C (dec). Anal. Calcd for C₆₂H₆₀N₂O₁₆P₄Pd₂Cl₄: C, 47.50; H, 3.86; N, 1.79. Found: C, 47.56; H, 3.79; N, 1.72%. ¹H NMR (400 MHz, CDCl₃): δ 8.02–6.78 (m, *Ph*, 36H), 3.62 (s, *OCH*₃, 24H). ³¹P{¹H} NMR (162 MHz, CDCl₃): δ 64.4 (s).

Synthesis of [Pt₂Cl₄- p -C₆H₄[N{P(OC₆H₄OMe-*o*)₂]₂]₂ (9**).** This was synthesized by a procedure similar to that of **8** using [Pt(COD)Cl₂] (0.025 g, 0.067 mmol) and **3** (0.042 g, 0.033 mmol). Yield: 81% (0.047 g). Mp: 240–244 °C. Anal. Calcd for C₆₂H₆₀N₂O₁₆P₄Pt₂Cl₄: C, 42.67; H, 3.47; N, 1.60. Found: C, 42.59; H, 3.44; N, 1.69%. ¹H NMR (400 MHz, CDCl₃): δ 8.03–6.83 (m, *Ph*, 36H), 3.60 (s, *OCH*₃, 24H). ³¹P{¹H} NMR (162 MHz, CDCl₃): δ 35.0 (s, ¹J_{PP} = 5072 Hz).

Synthesis of [Cu₄(μ -*Br*)₄(NCCH₃)₄- p -C₆H₄[N{P(OC₆H₄OMe-*o*)₂]₂]₂ (10**).** A solution of cuprous bromide (0.029 g, 0.205 mmol) in acetonitrile (5 mL) was added dropwise to a solution of **3** (0.062 g, 0.051 mmol) also in acetonitrile (5 mL). After stirring for 4 h, the solvent was concentrated under vacuum and kept at room temperature overnight to give analytically pure white crystals of **10**. Yield: 79% (0.079 g). Mp: > 240 °C (dec). Anal. Calcd for C₇₀H₇₂N₆O₁₆P₄Cu₄Br₄: C, 43.09; H, 3.72; N, 4.31. Found: C, 43.02; H, 3.70; N, 4.40%. ¹H NMR (400 MHz, CDCl₃): δ 7.66–6.75 (m,

Ph, 36H), 3.57 (s, *OCH*₃, 24H), 2.07 (s, *CH*₃CN, 12H). ³¹P{¹H} NMR (121 MHz, CDCl₃): δ 103.8 (br s).

Synthesis of [Cu₄(μ -*D*)₄(NCCH₃)₄- p -C₆H₄[N{P(OC₆H₄OMe-*o*)₂]₂]₂ (11**).** This was synthesized by a procedure similar to that of **10** using **3** (0.030 g, 0.025 mmol) and cuprous iodide (0.019 g, 0.099 mmol). Yield: 82% (0.044 g). Mp: 210–212 °C (dec). Anal. Calcd for C₇₀H₇₂N₆O₁₆P₄Cu₄I₄: C, 39.30; H, 3.39; N, 3.93. Found: C, 39.19; H, 3.30; N, 3.96%. ¹H NMR (400 MHz, CDCl₃): δ 7.74–6.75 (m, *Ph*, 36H), 3.55 (s, *OCH*₃, 24H), 2.07 (s, *CH*₃CN, 12H). ³¹P{¹H} NMR (121 MHz, CDCl₃): δ 102.6 (br s).

General Procedure for the Suzuki–Miyaura Cross-Coupling Reactions of Aryl Halides with Phenylboronic Acid. In a two-necked round-bottom flask under an atmosphere of nitrogen were placed the appropriate amounts of aryl halides (0.5 mmol), phenylboronic acid (0.75 mmol), K₂CO₃ (1 mmol), and 5 mL of methanol. After stirring for 2 min, 0.2 mol% of the catalyst [Pd₂Cl₄- p -C₆H₄[N{P(OC₆H₄OMe-*o*)₂]₂]₂ (**8**) was added. The mixture was stirred at room temperature or refluxed under an atmosphere of nitrogen, and the course of the reaction was monitored by GC analysis. After completion of the reaction, the solvent was removed under reduced pressure. The residual mixture was diluted with H₂O (10 mL) and extracted with Et₂O or toluene (2 × 6 mL). The combined organic fractions were dried (MgSO₄), stripped of the solvent under vacuum, and the residue was redissolved in 5 mL of dichloromethane. An aliquot was taken with a syringe and subjected to GC analysis. Conversions were calculated versus aryl halides as an internal standard.

X-ray Crystallography. A crystal of each of **1–3**, **6**, **7**, and **9–11** suitable for X-ray crystal analysis was mounted in a Cryolooop with a drop of Paratone oil and placed in the cold nitrogen stream of the Kryoflex attachment of the Bruker APEX CCD diffractometer. Full spheres of data were collected using a combination of three sets of 400 scans in ω (0.5° per scan) at $\varphi = 0, 90,$ and 180° plus two sets of 800 scans in φ (0.45° per scan) at $\omega = -30$ and 210° under the control of the SMART software package^{39a} (**1**, **3**, **6**, **7**, **9**) or the APEX2 program suite^{39b} (**2**). The crystals of **2** and **7** used for the structure determinations proved to be twinned, the former by a 180° rotation about the *a* axis and the latter by a 180° rotation about the *c* axis (CELL_NOW⁴⁰). The raw data were reduced to *F*² values using the SAINT+ software,⁴¹ and global refinements of unit cell parameters using 3036–9392 reflections chosen from the full data sets were performed. Multiple measurements of equivalent reflections provided the basis for empirical absorption corrections as well as corrections for any crystal deterioration during the data collection (SADABS^{42a} for **1**, **3**, **6**, **9** and TWINABS^{42b} for **2**, **7**). The structures were solved by direct methods (for **1–3**, **6**, **7**, and **9**) or the positions of the heavy atoms were obtained from a sharpened Patterson function (for **10** and **11**). All structures were refined by full-matrix least-squares procedures using the SHELXTL program package.⁴³ Hydrogen atoms were placed in calculated positions and included as riding contributions with isotropic displacement parameters tied to those of the attached non-hydrogen atoms.

(40) Sheldrick, G. M. CELL_NOW, University of Göttingen: Göttingen, Germany, 2005.

(41) SAINT+, versions 6.35A and 7.34A; Bruker-AXS: Madison, WI, 2002, 2006.

(42) (a) Sheldrick, G. M. SADABS, version 2.05 and version 2007/2; University of Göttingen: Göttingen, Germany, 2002, 2007. (b) Sheldrick, G. M. TWINABS, version 2007/5; University of Göttingen: Göttingen, Germany, 2007.

(43) (a) SHELXTL, version 6.10; Bruker-AXS: Madison, WI, 2000. (b) Sheldrick, G. M. SHELXS97 and SHELXL97; University of Göttingen: Göttingen, Germany, 1997.

Computational Details. The molecular structures of dimers of **1** and **2** were fully optimized using DFT. The calculations were performed in C_{2h} symmetry employing the PBE1PBE functional⁴⁴ in combination with the TZVP basis sets.⁴⁵ Full geometry optimizations were also performed for the C_{2h} symmetric model dimers $Cl_3P...PCl_3$ and $F_3P...PF_3$ at PBE1PBE and MP2⁴⁶ levels of theory using Dunning's triple- ζ quality basis sets augmented with polarization and diffuse functions (aug-cc-pVTZ) for all atoms.⁴⁷ Frequency calculations for the model systems were done only at the DFT level of theory. The correction of the basis set superposition error was done via the counterpoise procedure,⁴⁸ which was applied during geometry optimizations (MP2) and calculating binding energies (both DFT and MP2). All calculations were performed with the *Gaussian 03* program package.⁴⁹

Acknowledgment. We are grateful to the Department of Science and Technology (DST), New Delhi, for financial support of this work through grant SR/S1/IC-02/007. C.G. thanks CSIR, New Delhi, for a Senior Research Fellowship

(SRF). We also thank SAIF, Mumbai, Department of Chemistry Instrumentation Facilities, Bombay, for spectral and analytical data and J.T.M. thanks the Louisiana Board of Regents through grant LEQSF(2002-03)-ENH-TR-67 for the purchase of the CCD diffractometer and the Chemistry Department of Tulane University for support of the X-ray laboratory. H.M.T. thanks the Academy of Finland and the University of Jyväskylä for their generous financial support.

Supporting Information Available: X-ray crystallographic files in CIF format for the structure determinations of **1–3**, **6**, **7**, and **9–11**. This material is available free of charge via the Internet at <http://pubs.acs.org>.

IC800724U

- (44) (a) Perdew, J. P.; Burke, K.; Ernzerhof, M. *Phys. Rev. Lett.* **1996**, *77*, 3865–3868. (b) Perdew, J. P.; Burke, K.; Ernzerhof, M. *Phys. Rev. Lett.* **1997**, *78*, 1396. (c) Perdew, J. P.; Ernzerhof, M.; Burke, K. *J. Chem. Phys.* **1996**, *105*, 9982–9985. (d) Ernzerhof, M.; Scuseria, G. E. *J. Chem. Phys.* **1999**, *110*, 5029–5036.
- (45) (a) Schaefer, A.; Horn, H.; Ahlrichs, R. *J. Chem. Phys.* **1992**, *97*, 2571–2577. (b) Schaefer, A.; Huber, C.; Ahlrichs, R. *J. Chem. Phys.* **1994**, *100*, 5829–5835.
- (46) Møller, C.; Plesset, M. S. *Phys. Rev.* **1934**, *46*, 618–622.
- (47) Kendall, R. A., Jr.; Harrison, R. J. *J. Chem. Phys.* **1992**, *96*, 6796–6806.
- (48) Boys, S. F.; Bernardi, F. *Mol. Phys.* **1970**, *19*, 553–566.

- (49) Frisch, M. J.; Trucks, G. W.; Schlegel, H. B.; Scuseria, G. E.; Robb, M. A.; Cheeseman, J. R.; Montgomery, J. A., Jr.; Vreven, T.; Kudin, K. N.; Burant, J. C.; Millam, J. M.; Iyengar, S. S.; Tomasi, J.; Barone, V.; Mennucci, B.; Cossi, M.; Scalmani, G.; Rega, N.; Petersson, G. A.; Nakatsuji, H.; Hada, M.; Ehara, M.; Toyota, K.; Fukuda, R.; Hasegawa, J.; Ishida, M.; Nakajima, T.; Honda, Y.; Kitao, O.; Nakai, H.; Klene, M.; Li, X.; Knox, J. E.; Hratchian, H. P.; Cross, J. B.; Bakken, V.; Adamo, C.; Jaramillo, J.; Gomperts, R.; Stratmann, R. E.; Yazyev, O.; Austin, A. J.; Cammi, R.; Pomelli, C.; Ochterski, J. W.; Ayala, P. Y.; Morokuma, K.; Voth, G. A.; Salvador, P.; Dannenberg, J. J.; Zakrzewski, V. G.; Dapprich, S.; Daniels, A. D.; Strain, M. C.; Farkas, O.; Malick, D. K.; Rabuck, A. D.; Raghavachari, K.; Foresman, J. B.; Ortiz, J. V.; Cui, Q.; Baboul, A. G.; Clifford, S.; Cioslowski, J.; Stefanov, B. B.; Liu, G.; Liashenko, A.; Piskorz, P.; Komaromi, I.; Martin, R. L.; Fox, D. J.; Keith, T.; Al-Laham, M. A.; Peng, C. Y.; Nanayakkara, A.; Challacombe, M.; Gill, P. M. W.; Johnson, B.; Chen, W.; Wong, M. W.; Gonzalez, C.; Pople, J. A., *Gaussian 03, revision D.02*; Gaussian, Inc.: Pittsburgh, PA, 2003.